iScience

Article

Kremen1 regulates the regenerative capacity of support cells and mechanosensory hair cells in the zebrafish lateral line

heterozygous sibling zebrafish   krm1^nl10 mutant zebrafish

Sost+ dorsoventral support cell

Hair cell

BrdU+ cell

Poised projenitor cell

Neomysin hair cell ablation

Regeneration

Sost+ BrdU+ Hair cell

Sost+ BrdU- Hair cell

Posterior lataral line neuromasts

Ellen Megerson, Michael Kuehn, Ben Leifer, Jon M. Bell, Julia L. Snyder, Hillary F. McGraw

mcgrawh@umkc.edu

Highlights

Kremen1 mutants have supernumerary lateral line hair cell development and regeneration

Supernumerary hair cell regeneration occurs independently of changes in proliferation

Dorsoventral support cells are expanded in Kremen1 mutant lateral line neuromasts

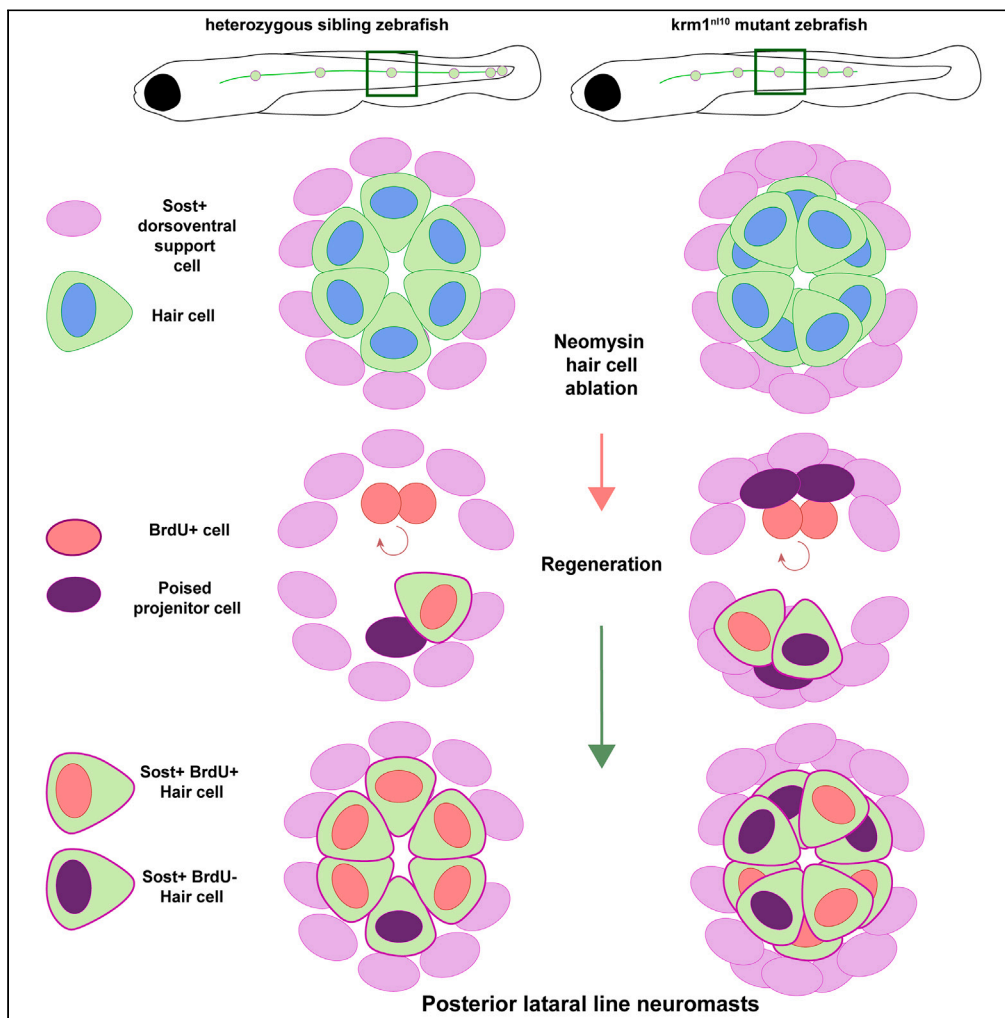Wnt signaling regulates poised hair cell progenitors in the lateral line

Article

Kremen1 regulates the regenerative capacity of support cells and mechanosensory hair cells in the zebrafish lateral line

Ellen Megerson,[1,2] Michael Kuehn,[1,3] Ben Leifer,[1,4] Jon M. Bell,[1] Julia L. Snyder,[1] and Hillary F. McGraw[1,5,*]

SUMMARY

Mechanosensory hair cells in the inner ear mediate the sensations of hearing and balance, and in the specialized lateral line sensory system of aquatic vertebrates, the sensation of water movement. In mammals, hair cells lack the ability to regenerate following damage, resulting in sensory deficits. In contrast, non-mammalian vertebrates, such as zebrafish, can renew hair cells throughout their lifespan. Wnt signaling is required for development of inner ear and lateral line hair cells and regulates regeneration. Kremen1 inhibits Wnt signaling and hair cell formation, though its role in regeneration is unknown. We used a zebrafish *kremen1* mutant line to show overactive Wnt signaling results in supernumerary support cells and hair cell regeneration without increased proliferation, in contrast with the previously described role of Wnt signaling during hair cell regeneration. This work allows us to understand the biology of mechanosensory hair cells and how regeneration might be promoted following damage.

INTRODUCTION

Loss of hearing is one of the most common sensory defects found among the human population as an estimated 15% of the world's population has some degree of hearing loss and over 5% have disabling loss of auditory function (https://www.who.int/news-room/fact-sheets/detail/deafness-and-hearing-loss). Hearing, along with vestibular function, is mediated by specialized mechanosensory hair cells found within the inner ear. In mammals, hair cells damaged through exposure to noise, ototoxic drugs, injury, or disease fail to regrow.[1–5] By contrast, non-mammalian vertebrates, such as chickens, frogs, and fish, are capable of regenerating hair cells, often throughout their lifespan.[6–8] Understanding how hair cells regenerate in some animals is critical to identifying potential therapies for human hearing loss.

In addition to inner ear hair cells, aquatic vertebrates have mechanosensory hair cells in their lateral line sensory systems that mediate sensations of water movement.[9] Lateral line hair cells are morphologically and genetically very similar to the inner ear hair cells of the auditory and vestibular systems.[10] The lateral line is arrayed on the surface of the body and amenable to manipulation, unlike the inner ear, which is difficult to access and experimentally manipulate.[11,12] The zebrafish (*Danio rerio*) has emerged as an excellent model organism for the study of mechanosensory hair cell development and regeneration.[13] Neuromasts are the sensory organs of the lateral line and are composed of mechanosensory hair cells to sense water movement and surrounding support cells, which maintain neuromast homeostasis by acting as stem cells.[14] In the zebrafish, lateral line hair cells are robustly regenerative throughout the life of the animal.[6]

Recent work determined specific subpopulations of neuromast support cells preferentially give rise to regenerated hair cells, self-renew to maintain stem cell numbers, or remain quiescent under most conditions.[15–19] Single-cell RNA-sequencing identified specific gene expression profiles for the distinct subpopulations of neuromast support cells during neuromast regeneration.[15,16,18,20] The transcriptional profiles served as the basis for cell labeling experiments to analyze the behavior of support cells as hair cells are regrown. In particular, the *Tg(sost:nlsEos)^w215* transgenic line allowed conditional labeling of dorsoventral support cells and demonstrated these cells proliferate to give rise to the majority of hair cells during regeneration.[19] The proliferation of anterior-posterior support cells labeled with the *Tg(tnfs10L3:nlsEos)^w218* formed the minority of regenerating hair cells and primarily gave rise to self-renewing support cells. Finally, peripheral support cells labeled with *Tg(sfrp1a:nlslEos)^w217* were largely quiescent, though extensive ablation of interior support cells can trigger peripheral support cells to proliferate and repopulate the neuromast.[19,21,22] As we gain a better understanding of how specific populations of support cells contribute to regeneration, the question is raised: how are these cell populations specified?

Fgf, Notch and Wnt signaling regulate proliferation and regeneration in the zebrafish lateral line.[16,23–26] Regulation of the Fgf and Notch pathways are required for the maintenance of proper hair cell numbers by inhibiting support cell proliferation and hair cell differentiation

under homeostatic conditions. Following hair cell ablation, blocking the function of either Fgf or Notch during neuromast regeneration, via pharmacological antagonists or mutant zebrafish lines, results in increased support cell proliferation and differentiation of supernumerary hair cells.[16,19,24] Analysis of support cell subpopulations found Notch signaling inhibition increased regenerated hair cells forming from dorsoventral and anterior-posterior populations. In particular, anterior-posterior cells labeled with *Tg(tnfs10L3:nlsEos)*[w218] contributed to a greater proportion of regenerated hair cells as compared to control regeneration conditions.[19]

Canonical Wnt signaling has been implicated as a critical pathway regulating neuromast regeneration in the zebrafish lateral line. Gene expression patterns and single cell RNA-sequencing examined during neuromast regeneration revealed canonical Wnt signaling is upregulated beginning 3 h after hair cell ablation and remains active during the first 10h of regeneration.[15,16,24] Studies using pharmacological manipulation of the Wnt pathway or overexpression of pathway inhibitors such as heat-shock induction of Dkk1b, suggest Wnt signaling is required for the proliferation of support cells and hair cell regeneration.[16,24,27] Our current study is the first to specifically examine neuromast regeneration in a zebrafish Wnt pathway mutant.

Kremen1 (Krm1) is a vertebrate-specific member of the Wnt pathway which inhibits Wnt signaling as a co-receptor for the secreted family of Dkk proteins.[28,29] In the mouse cochlea, *krm1* is expressed in support cells and inhibiting Krm1 function in cochlear explants results in the formation of excess and disordered hair cells, but not significant changes in proliferation.[30] In zebrafish, a *krm1* mutant line (*krm1*[nl10]) shows truncated posterior lateral line formation and an increase in the development of neuromast hair cells.[30,31] Blocking *krm1* function with a morpholino, resulted in the development of physically larger neuromasts, but no significant change in hair cell number.[32] A role for Krm1 function in hair cell regeneration has not been investigated.

In this study, we use the *krm1*[nl10] zebrafish mutant line to determine the role of Krm1 in the regulation of cellular behavior during regeneration in the zebrafish posterior lateral line. Our analysis of hair cell numbers following ablation and regeneration shows a significant increase in *krm1*[nl10] mutants, though not an increase in cellular proliferation. Instead, we find loss of Krm1 function results in an increase of *Tg(sost:nlsEos)*[w215] labeled dorsoventral support cells, which give rise to regenerated hair cells. We can eliminate the supernumerary hair cells in *krm1*[nl10] larvae following repeated bouts of regeneration, suggesting a poised population of support cells exists which can be overwhelmed by repeated regeneration. Finally, we demonstrate Notch signaling inhibition increases cellular proliferation, resulting in greater numbers of dorsoventral support cells and regenerated hair cells in *krm1*[nl10] mutant larvae. Overall, our results suggest regulation of Krm1 function is required for proper hair cell renewal after damage.

RESULTS

krm1 is dynamically expressed during regeneration in posterior lateral line NMs

Previous research revealed expression of *krm1* in migrating posterior lateral line primordium during the initial 48 h of development in the zebrafish embryo and in the support cells of developing adult mouse cochlea.[30,31] We used whole-mount RNA *in situ* hybridization (WISH)[33] and hybridization chain reaction (HCR)[34,35] for fluorescent *in situ* hybridization (FISH) to examine the expression patterns of *krm1* in the zebrafish lateral line during regeneration. At 5 days post fertilization (dpf) *krm1* is expressed throughout the neuromast (Figure 1A), when Wnt signaling is expected to be low.[24] We used neomycin (*NEO*) to ablate hair cells and induce regeneration. We examined the expression pattern of *krm1* in neuromasts at 4 h post *NEO* (Figure 1B), when Wnt is upregulated[15,16,24] and 1 day post *NEO* (Figure 1C). At these time points, *krm1* expression is greatly reduced. By 3 days post *NEO*, regeneration is complete and *krm1* expression is again expressed in neuromasts (Figure 1D).

Building on the dynamic expression of *krm1* during regeneration, we next sought to determine if there is cell-specific localization of *krm1* in NMs. By examining HCR-FISH in *Tg(myosin6b:GFP)*[w186] (*myo6:GFP*) expressing larvae at 5dpf, we found *krm1* is expressed throughout the neuromast in surrounding support cells and *myo6:GFP*-positive hair cells (Figures 1E–1E′′′ and 1I). In agreement with our WISH experiments, at 4 h post NEO-exposure we observe a significant decrease in HCR *krm1* expression (Figures 1F–1F′′′ and 1I) and a moderate recovery of expression by 1 day post *NEO* (Figures 1G–1G′′′ and 1I). By 3 -days after NEO-exposure, HCR *krm1* expression has returned to homeostatic levels in regenerated NMs (Figures 1H–1H′′′ and 1I). Together our results indicate *krm1* expression is present during homeostasis in NMs when Wnt signaling is low and downregulated during regeneration when Wnt signaling is upregulated.

Supernumerary hair cells form during regeneration in *krm1*[nl10] mutants

During development, Krm1 is expressed in the support cells of the mouse cochlea.[30] Blockage of Krm1 function by RNAi results in a significant increase in the number of cochlear hair cells, though without a change in levels of proliferation.[30] Examination of the *krm1*[nl10] zebrafish mutant line also showed an increase in the number of lateral line hair cells during development.[30] We sought to determine if Krm1 activity also regulates the regeneration of hair cells in the zebrafish posterior lateral line. At 5dpf, prior to hair cell ablation with *NEO*, *krm1*[nl10] mutant larvae have significantly more hair cells labeled with *myo6:GFP* as compared to heterozygous and wild-type siblings (Figures 2A, 2A′, 2B, 2B′, and 2G). Total cell numbers as labeled by DAPI and α-Sox2 antibody-labeled support cells and hair cells within NMs did not show a significant change between mutants and heterozygous sibling control larvae (Figures 2A′′–2B′′′, 2H, and 2I). To confirm hair cells are susceptible to *NEO* damage, we examined control and *krm1*[nl10] NMs 1 h post exposure to *NEO* and found the majority of hair cells were ablated (Figures 2C–2D′′′ and 2G). To assess regeneration, we quantified hair cell numbers 3 days post *NEO* exposure and found a significant increase in *myo6:GFP*+ cells in *krm1*[nl10] mutants as compared to heterozygous siblings (Figures 2E–2F′ and 2G). However, support cells and total cell numbers were not significantly different (Figures 2E′′–2F′′′, 2H, and 2I). We also compared the percentage of hair cell numbers to total cells within NMs to confirm that the differences we are seeing are not the result of changes in overall neuromast size and still find a significant
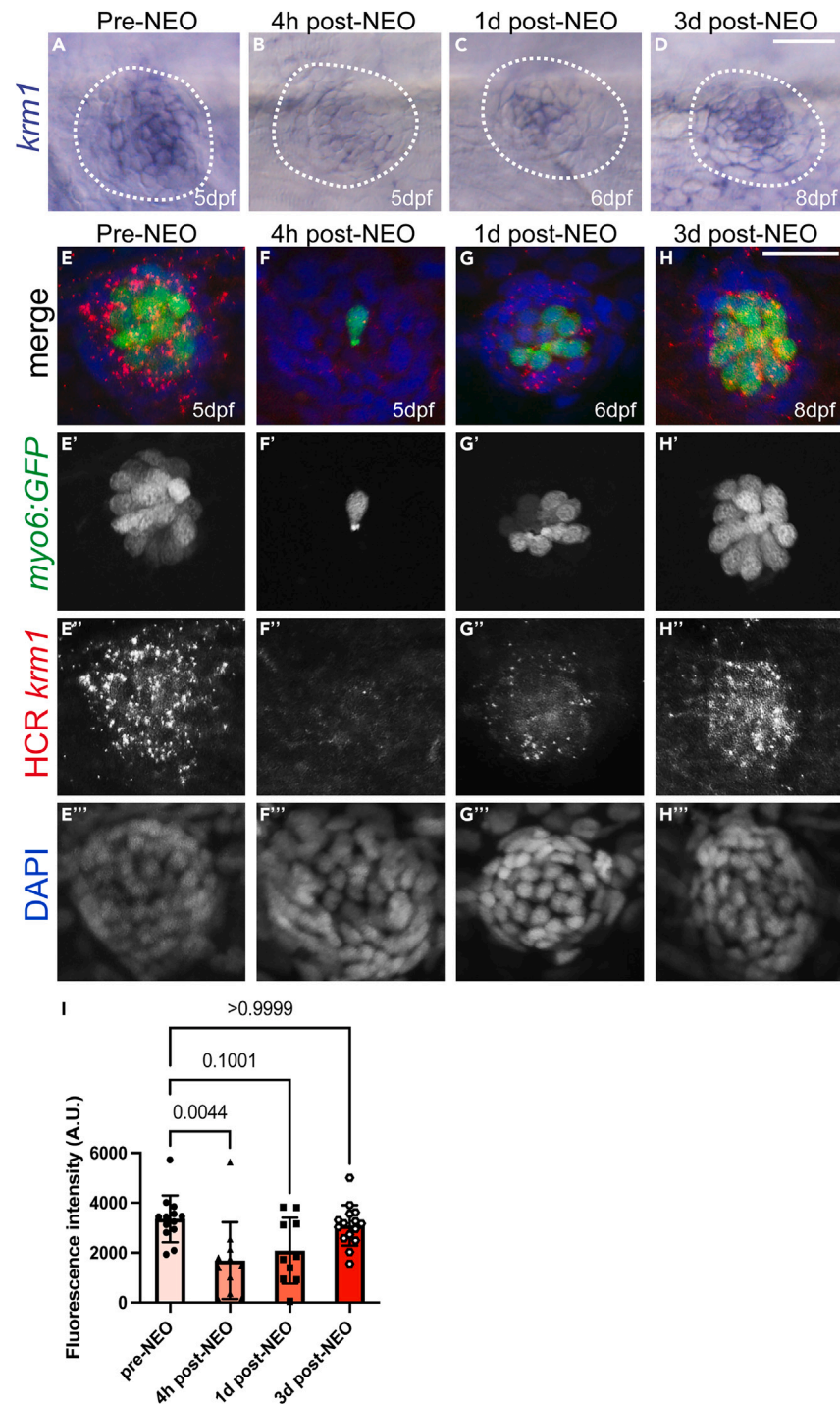
Figure 1. *krm1* **expression is dynamic during posterior lateral line regeneration**

(A–D) RNA *in situ* hybridization of *krm1* showing expression in 5dpf NM prior to exposure to *NEO*, 4 h after *NEO* exposure, 1 day post *NEO* exposure in a 6dpf larva, and 3 -days post *NEO* exposure in 8dpf larva.

(E–H) Confocal projections of HCR-FISH showing *krm1* expression (red) during regeneration in wild-type NMs in *Tg(myosin6b:GFP)^{w186}* larvae (green) with nuclei labeled with DAPI (blue) in 5dpf NM prior to exposure to *NEO*, 4 h after *NEO* exposure, 1 day post *NEO* exposure in a 6dpf larva, and 3 days post *NEO* exposure in a 8dpf larva.

(I) Quantification of fluorescence intensity in arbitrary units (A.U.) of HCR *krm1* expression normalized to background during regeneration in wild-type larvae. Pre-NEO n = 13 NM (7 fish), 4 h post-NEO n = 11 NM (7 fish), 1 day post-NEO n = 10 NM (7 fish), and 3 days post-NEO n = 14 NM (9 fish).

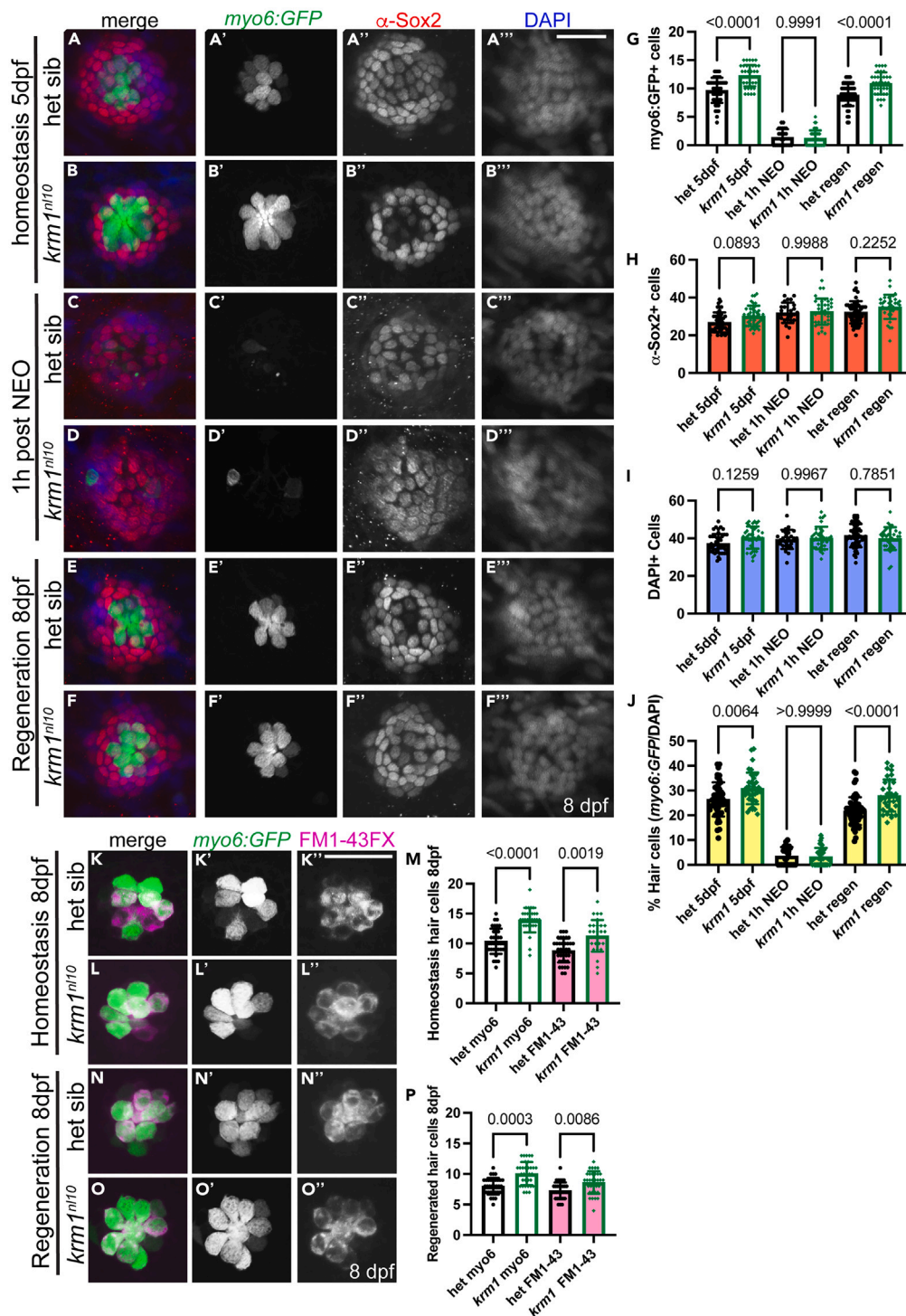All data presented as mean ± SD, Kruskal-Wallis test, Dunn's multiple comparisons test. Scale bar = 20 μm.

Figure 2. *krm1^nl10* larvae form supernumerary hair cells following regeneration in posterior lateral line neuromasts

(A–B‴) Confocal projections of neuromasts in heterozygous sibling and *krm1^nl10* larvae with *Tg(myosin6b:GFP)^w186* expression in hair cells (green), α-Sox2 antibody-labeled support cells (red) and DAPI-labeled nuclei (blue) at 5dpf NM prior to exposure to *NEO*.

(C–D‴) Heterozygous sibling and *krm1^nl10* mutant at 1 h post *NEO* exposure.

(E–F‴) Heterozygous sibling and *krm1^nl10* mutant 3 days post *NEO* exposure.

(G–J) Quantification of *Tg(myosin6b:GFP)^w186* positive hair cells, α-Sox2 antibody-labeled support cells at 5dpf pre-NEO exposure, and the percentage of hair cells *Tg(myosin6b:GFP)^w186*-positive cells/DAPI-labeled cells) at 1-h post *NEO* exposure, and at 8dpf, 3 days post *NEO* exposure.). 5dpf: het sibling n = 48 NMs

difference in homeostatic and regenerated hair cells in *krm1^nl10* mutants as compared to heterozygous siblings (Figure 2J). These results suggest mechanisms leading to excess hair cell number during development in *krm1^nl10* mutants may also regulate hair cell regeneration.

We next sought to confirm the supernumerary hair cells found in *krm1^nl10* mutants have functional mechanoelectrical transduction (MET) channels by using the vital dye FM1-43FX which enters the cell through functional MET channels.[36,37] Significantly more hair cells are labeled with FM1-43 at 8dpf in *krm1^nl10* mutant NMs under both homeostatic and regeneration conditions as compared to heterozygous siblings (Figures 2K–2P). These results suggest the supernumerary hair cells in *krm1^nl10* mutants have the potential for functional signaling.

Wnt activity is responsible for excess hair cells in regenerating *krm1^nl10* mutant NMs

The canonical Wnt signaling pathway is activated during hair cell regeneration in the zebrafish lateral line.[24] Single-cell RNA sequencing studies have demonstrated Wnt signaling is upregulated beginning 3 h after hair cell ablation with *NEO* in the zebrafish lateral line.[15,16] To assess Wnt signaling dynamics during regeneration in our *krm1^nl10* line, we examined the expression of *β-catenin b1* (*ctnnb1*) and *wnt2* by WISH. In 5dpf larvae, prior to NEO-exposure, we found low levels of *ctnnb1* and *wnt2* expression in wild-type and mutant NMs (Figures 3A, 3B, 3E, and 3F) and increased expression of both RNAs at 4 h post *NEO* in wild-type and *krm1^nl10* mutant larvae (Figures 3C, 3D, 3G, and 3H). We conclude Wnt signaling is active during regeneration in control and *krm1^nl10* NMs.

We next sought to determine if altering Wnt activity pharmacologically results in changes in regenerated hair cell numbers *krm1^nl10* mutant larvae. Previous work demonstrated altered regeneration patterns in the lateral line with exposure to Wnt signaling activators resulting in increased hair cell numbers or Wnt inhibitors resulting in fewer hair cells.[13] We exposed heterozygous sibling and *krm1^nl10* mutant larvae to the Wnt inhibitor IWR-1 or the Wnt activator 1-azakenpaullone (AZK[38]) following NEO-induced hair cell ablation and quantified the number of hair cells (Figure 3I). Larvae exposed to DMSO regenerated supernumerary α-Otoferlin-antibody labeled hair cells in *krm1^nl10* mutant NMs relative to heterozygous sibling larvae (Figures 3J, 3K, and 3N). Exposure to IWR-1 produced a trend toward decreased regenerated hair cells in heterozygous and a significant decrease in *krm1^nl10* NMs as compared to DMSO treated larvae (Figures 3L, 3M, and 3N). Though, *krm1^nl10* mutants showed significantly more regenerated hair cells than heterozygous siblings following IWR-1 exposure (Figure 3N), suggesting the inhibitor does not entirely block Wnt activity. In a reciprocal experiment, larvae were exposed to AZK during regeneration to overactivate Wnt signaling. We found exposure to AZK during regeneration resulted in a significant increase in the number of hair cells in heterozygous sibling NMs as compared to DMSO controls (Figures 3O, 3Q, and 3S), but no significant change in hair cell numbers in *krm1^nl10* mutant larvae as compared to DMSO treated *krm1^nl10* larvae or AZK-exposed heterozygous controls (Figures 3P, 3R, and 3S). Together the results suggest loss of Krm1 function results in increased Wnt signaling during regeneration in the posterior lateral line and leads to the formation of supernumerary hair cells. Blocking Wnt signaling with IWR-1 reduces the bias toward hair cell formation in *krm1^nl10* mutants, while further activating Wnt with AZK results in increase hair cell regeneration in control larvae, but not mutants.

Regenerative proliferation is not increased in *krm1^nl10* mutant larvae

Previous work using chemical Wnt inhibitor and overexpression models, suggested Wnt signaling regulates the proliferation of NM support cells in response to hair cell ablation.[13,39,40] Inhibition of Wnt signaling using IWR-1 or conditional overexpression of Dkk family members, resulted in a decrease in proliferation during regeneration. Conversely, treatment with Wnt activators LiCl, BIO or AZK, resulted in an increase in proliferation during regeneration.[13,16,24–27,39,41,42] We sought to replicate the experiments by examining BrdU incorporation in DMSO, IWR-1 or AZK exposed larvae during regeneration (Figure S1A). Consistent with previous work, we found altering Wnt signaling with IWR-1 results in a significant decrease in proliferation (Figures S1B–C″, S1E, and S1F) and AZK results in a significant increase in proliferation during NM regeneration (Figures S1B–B″, S1D–S1D″, and S1E).

To determine if loss of Krm1 function alters proliferation in a similar manner during hair cell regeneration, we performed a set of pulse-chase BrdU incorporations during the 3-day period of regeneration following exposure to *NEO* (Figure 4A). Cells in regenerating NMs primarily incorporate BrdU during the first day following hair cell ablation.[22] Following BrdU incorporation during 5-6dpf, we did not find a significant difference in the number of BrdU-positive cells at 8dpf in control or *krm1^nl10* larvae (Figures 4B–C‴ and 4H). We also found the percentage of BrdU+ cells compared to total DAPI+ (Figure 4I) and the percentage of BrdU+ hair cells (Figure 4J) were not significantly different in *krm1^nl10* mutants as compared to heterozygous sibling controls. To determine if proliferation is delayed in *krm1^nl10* during regeneration, we exposed regenerating larvae to BrdU during 6-7dpf (Figures 4D–4E‴) or 7-8dpf (Figures 4F–4G‴) following NEO-exposure at 5dpf and then collected the larvae at 8dpf when regeneration was complete. We found no significant change in the total cells incorporating BrdU (Figure 4H) or in the percentage
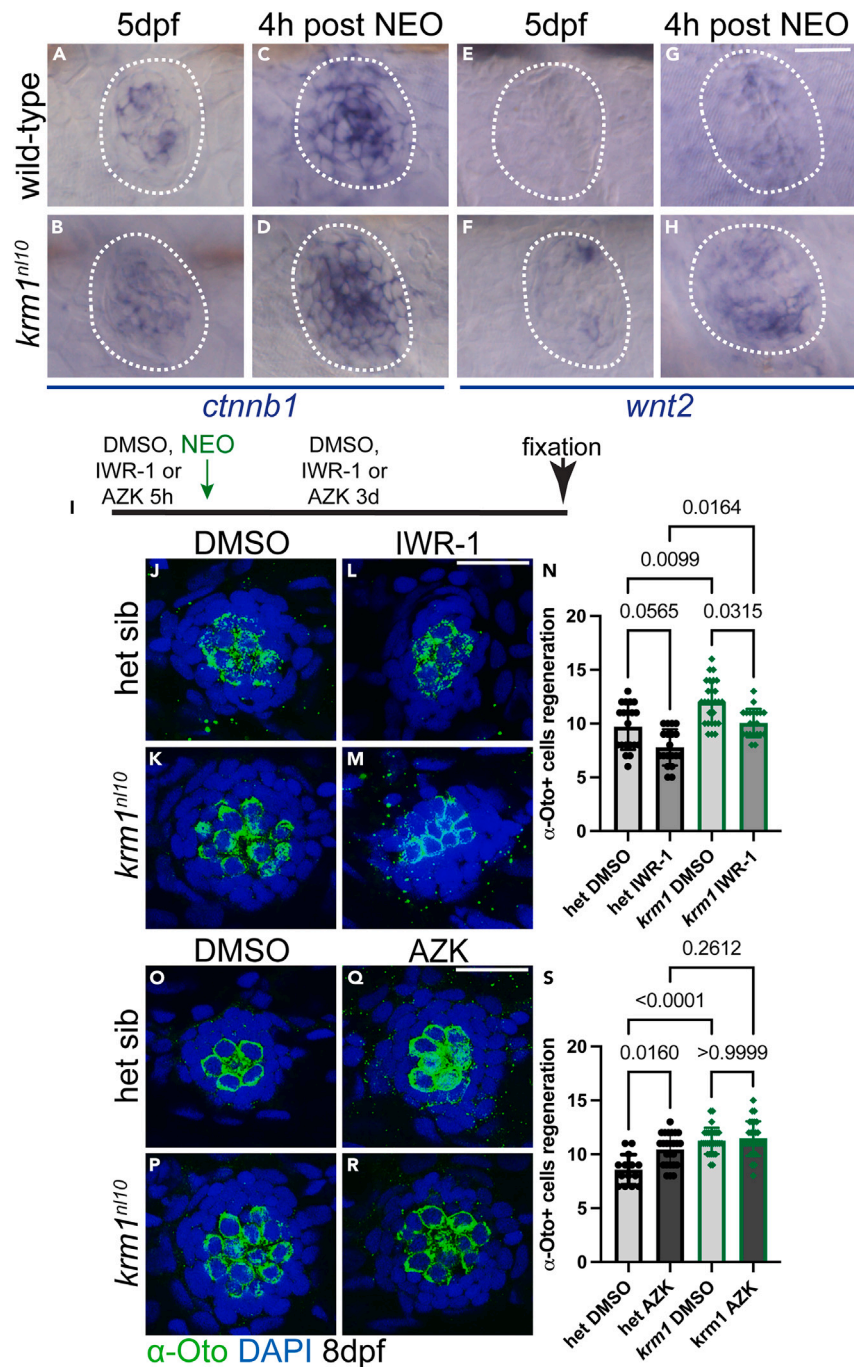
Figure 3. Wnt signaling is active during regeneration in *krm1^nl10* neuromasts

(A–D) Representative images of RNA *in situ* hybridization at 5dpf of *ctnnb1* expression in wild-type and *krm1^nl10* mutant NMs without exposure to *NEO* and 4 h post *NEO* exposure.

(E–H) *wnt2* expression in wild-type and *krm1^nl10* mutant NMs without exposure to *NEO* and 4 h post *NEO* exposure. Scale bar = 20 μm.

(I) Timeline of DMSO or inhibitor exposure, NEO-induced hair cell ablation, and regeneration between 5dpf and 8dpf.

(J–M) Confocal projects of 8dpf NMs following regeneration, hair cells are labeled with α-Otoferlin antibody (green) and nuclei are labeled with DAPI (blue) in heterozygous sibling or *krm1^nl10* NMs with exposure to DMSO or IWR-1.

(N) Quantification of α-Otoferlin-positive cells. DMSO-exposed heterozygous sibling n = 20 NM (8 fish) and IWR-1-exposed heterozygous sibling n = 19 NM (9 fish), and DMSO-exposed) and IWR-1-exposed *krm1^nl10* n = 20 NM (9 fish).

Figure 3. Continued

(O–R) Confocal projects of 8dpf NMs following regeneration, hair cells are labeled with α-Otoferlin antibody (green) and nuclei are labeled with DAPI (blue) in heterozygous sibling or $krm1^{nl10}$ NMs with exposure to DMSO or AZK.

(S) Quantification of α-Otoferlin-positive cells. DMSO-exposed heterozygous sibling n = 14 NM (8 fish) and DMSO-exposed $krm1^{nl10}$ n = 29 NM (9 fish), and AZK-exposed heterozygous sibling n = 26 NM (11 fish) and AZK-exposed $krm1^{nl10}$ n = 28 NM (9 fish). All data presented as mean ± SD, Kruskal-Wallis test, Dunn's multiple comparisons test. Scale bar = 20 μm. See also Figure S1.

of total cells (Figure 4I) or hair cells which incorporated BrdU (Figure 4J). Together our analyses of BrdU incorporation suggest the increase in hair cells present in $krm1^{nl10}$ mutants following regeneration are not the result of increased proliferation in NM cells.

Repeated regeneration eliminates supernumerary hair cells in $krm1^{nl10}$ mutant NMs

The absence of increased proliferation in $krm1^{nl10}$ mutants leads us to speculate there may be a population of support cells poised to replenish lost hair cells in posterior lateral line NMs which do not rely on entry into the cell cycle. We reasoned, if such a population of cells exists, repeated regeneration might be sufficient to reduce their number in $krm1^{nl10}$ mutant larvae thus eliminating the potential to form supernumerary hair cells (Figure 5A). We assessed hair cell number at 8dpf following exposure to *NEO* at 5dpf and 3 days of regeneration (1x *NEO*; Figures 5B–5C′ and 5J), at 11dpf after 2 rounds of regeneration (2x *NEO*; Figures 5D–5E′ and 5J), at 14dpf after 3 rounds of regeneration (3x *NEO*; Figures 5F–5G′ and 5J), and at 17dpf after 4 rounds of regeneration (4x *NEO*; Figures 5H–5I′ and 5J). As expected from our previous experiments, we found $krm1^{nl10}$ NMs formed significantly more hair cells compared to heterozygous siblings following the first round of regeneration (Figure 5J). However, in each subsequent exposure to *NEO* and regeneration, we found no significant differences in the number of regenerated hair cell between mutant and control larvae (Figure 5J). We also examined total NM cell numbers using DAPI labeling of nuclei and did not find significant differences between heterozygous sibling and $krm1^{nl10}$ mutant larvae during the repeated rounds of regeneration (Figures 5B″–5I″ and 5K).

To confirm the change in regeneration patterns we see with repeated exposure to *NEO* is based specifically on the response to damage rather than age of the larvae, we exposed 14dpf larvae to *NEO* and assessed regeneration at 17dpf (Figure 5L). This single round to regeneration in older larvae again resulted in significantly more regenerated hair cells in $krm1^{nl10}$ mutant NMs (Figures 5N–5N‴ and 5O) as compared to heterozygous siblings (Figures 5M–M‴ and 5O), though no difference in DAPI+ cells (Figure 5P), indicating age is not the cause of the absence of supernumerary hair cells following repeated damage.

To determine if the poised population of support cells found $krm1^{nl10}$ can be re-established following damage, we performed two rounds of hair cell ablation separated by a period of recovery. We exposed heterozygous sibling and $krm1^{nl10}$ larvae to *NEO* at 5dpf, then allowed them to recover until 14dpf, at which time we performed a second *NEO* exposure and assessed hair cell regeneration at 17dpf (Figure 5Q). We found in contrast to immediately successive rounds of regeneration, a period of recovery re-established the formation of supernumerary hair cells in $krm1^{nl10}$ mutant NMs (Figures 5R–5U). Together these experiments suggest there is a population of support cells in $krm1^{nl10}$ mutants biased to give rise to hair cells which can be depleted by frequent repeated regenerations.

Dorsoventral support cells are increased in $krm1^{nl10}$ mutant neuromasts

Recent studies have found distinct subpopulations of support cells within lateral line NMs that preferentially contribute to hair cell regeneration ([16,19,20]). We sought to determine if specific support cell populations are altered in $krm1^{nl10}$ mutant larvae during development. We began by examining *sost* expression in dorsoventral support cells (Figures 6A and 6B) and found a small increase in $krm1^{nl10}$ mutants compared with heterozygous siblings. We then quantified photoconverted $Tg(sost:nlsEos)^{w215}$-expressing dorsoventral support cells and *myo6:GFP*-expressing hair cells in heterozygous sibling (Figures 6C–6C″) and $krm1^{nl10}$ mutant NMs (Figures 6D–6D″) at 5dpf. We found significantly more *myo6:GFP*+ and *sost:nlsEos*+ cells in mutant larvae as compared to heterozygous siblings at 5dpf (Figures 6E and 6F). We also examined other support cell subpopulations. We found no significant difference between heterozygous siblings and $krm1^{nl10}$ mutant NMs in *tnfsf10L3*-expressing apical-basal support cells using WISH and HCR-FISH (Figures S2A–S2E) nor *sfrp1a*-expressing peripheral support cells using WISH and $Tg(sfrp1a:nlsEos)^{w217}$ (Figures S2F–S2J).[19] Central supports cells were examined using WISH for *six1a*, *lfng*, and *isl1a*, and did not show appreciably different expression patterns in heterozygous larvae and $krm1^{nl10}$ mutants (Figures S2K–S2P).[15,16,20] Together the results suggest loss of Krm1 function during development results in an increase of dorsoventral support cells, as well as the differentiation of hair cells in the posterior lateral line without an increase in overall NM size.

Dorsoventral cell contribute to the regeneration of supernumerary hair cells in $krm1^{nl10}$ NMs

To analyze the contribution of *sost:nlsEos*+ support cells to hair cell regeneration, we photoconverted $Tg(sost:nlsEos)^{w215}$ larvae, which also carried the $Tg(myosin6b:GFP)^{w186}$ transgene, by exposure to UV light at 5dpf and assessed cell numbers at 8dpf in live larvae. Under homeostatic conditions (Figure 7A), we find significantly more photoconverted *sost:nlsEos*+ dorsoventral support cells and *myo6:GFP*+ hair cells in $krm1^{nl10}$ mutant NMs (Figures 7C–7C″, 7D and 7E) as compared to heterozygous siblings (Figures 7B–7B″, 7D and 7E). However, we did not find a significant change in the hair cells co-expressing *myo6:GFP* and *sost:nlsEos* (Figure 7F), suggesting under homeostatic conditions, few hair cells arise between 5-8dpf. To assess the contribution of *sost:nlsEos*+ dorsoventral support cells to hair cell regeneration, we exposed larvae to *NEO* following photoconversion at 5dpf and allowed regeneration to progress to 8dpf before live imaging (Figure 7G). Under regeneration conditions, we found a significant increase in total *myo6:GFP*+ hair cells, hair cells expressing
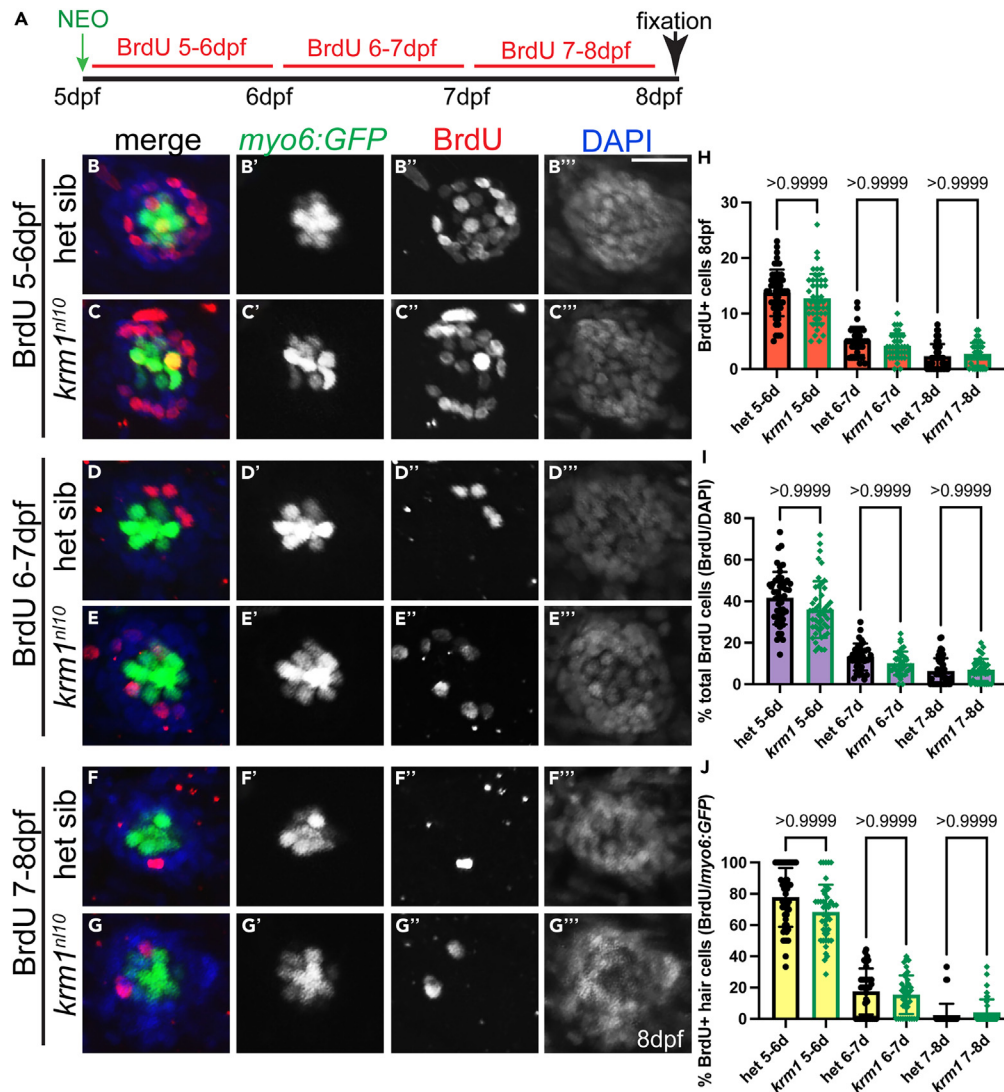
Figure 4. Proliferation does not contribute to the regeneration of supernumerary hair cells in *krm1*[nl10] neuromasts

(A) Timeline of neomycin expose at 5dpf, followed by 24 h of BrdU incubation at 5-6dpf, 6-7dpf, or 7-8dpf, all conditions were allowed to develop until 8dpf then fixed and processed for imaging.

(B–G‴′'') Confocal projections of L2 neuromasts at 8dpf expressing *Tg(myosin6b:GFP)*[w186] to label regenerated hair cells (*myo6:GFP*; green), BrdU incorporation (red), and DAPI labeling of nuclei (blue) at 5-6dpf in heterozygous sibling or *krm1*[nl10] mutant neuromasts NMs, from 6-7dpf,or from 7-8dpf. Scale bar = 20 μm.

(H–J) Total numbers of BrdU-positive cells in heterozygous or *krm1*[nl10] mutant neuromasts, percentage of total BrdU-positive cells (total BrdU+ cells/total DAPI+ cells), and percentage of BrdU-positive hair cells (BrdU+ *myo6:GFP*+ cells/total *myo6:GFP*+ cells). 5-6dpf: het sibling n = 50 NMs (12 fish), *krm1*[nl10] n = 46 NM (11 fish); 6-7dpf: het sibling n = 34 NMs (9 fish), *krm1*[nl10] n = 39 NM (9 fish); 7-8dpf: het sibling n = 50 NMs (12 fish), *krm1*[nl10] n = 40 NM (10 fish). All data presented as mean ± SD, Kruskal-Wallis test, Dunn's multiple comparisons test.

myo6:GFP and *sost:nlsEos*, and total *sost:nlsEos*+ cells in *krm1*[nl10] mutant NMs (Frig. 7I-I″,J,K,L) as compared to heterozygous control larvae (Figures 7H–7H″, 7J, 7K and 7L). These results suggest the supernumerary *sost:nlsEos*+ support cells in *krm1*[nl10] mutants give rise to excess hair cells during regeneration. We next asked if repeated regeneration could overwhelm *sost:nlsEos*+ dorsoventral support cells and reduce the number of regenerated hair cells. Building on our finding that two rounds of damage was sufficient to eliminate supernumerary hair cells in *krm1*[nl10] mutants (Figure 5), we performed photoconversion and *NEO* exposure on *sost:nlsEos* and *myo6:GFP* larvae at 5dpf and again at 8dpf for two rounds of regeneration before collection and live imaging at 11dpf (Figure 7M). We no longer found a significant difference in the total number of regenerated *myo6:GFP*+ hair cells, hair cells co-expressing *myo6:GFP* and *sost:nlsEos*, or total *sost:nlsEos*+ support cells between heterozygous siblings (Figures 7N–7N″ and 7P–7R) and *krml*[nl10] mutant larvae (Figures 7O–7O″ and 7P–7R). Together with our previous results, these findings suggest a population of dorsoventral support cells are the source of supernumerary hair cells in *krm1*[nl10] mutants.
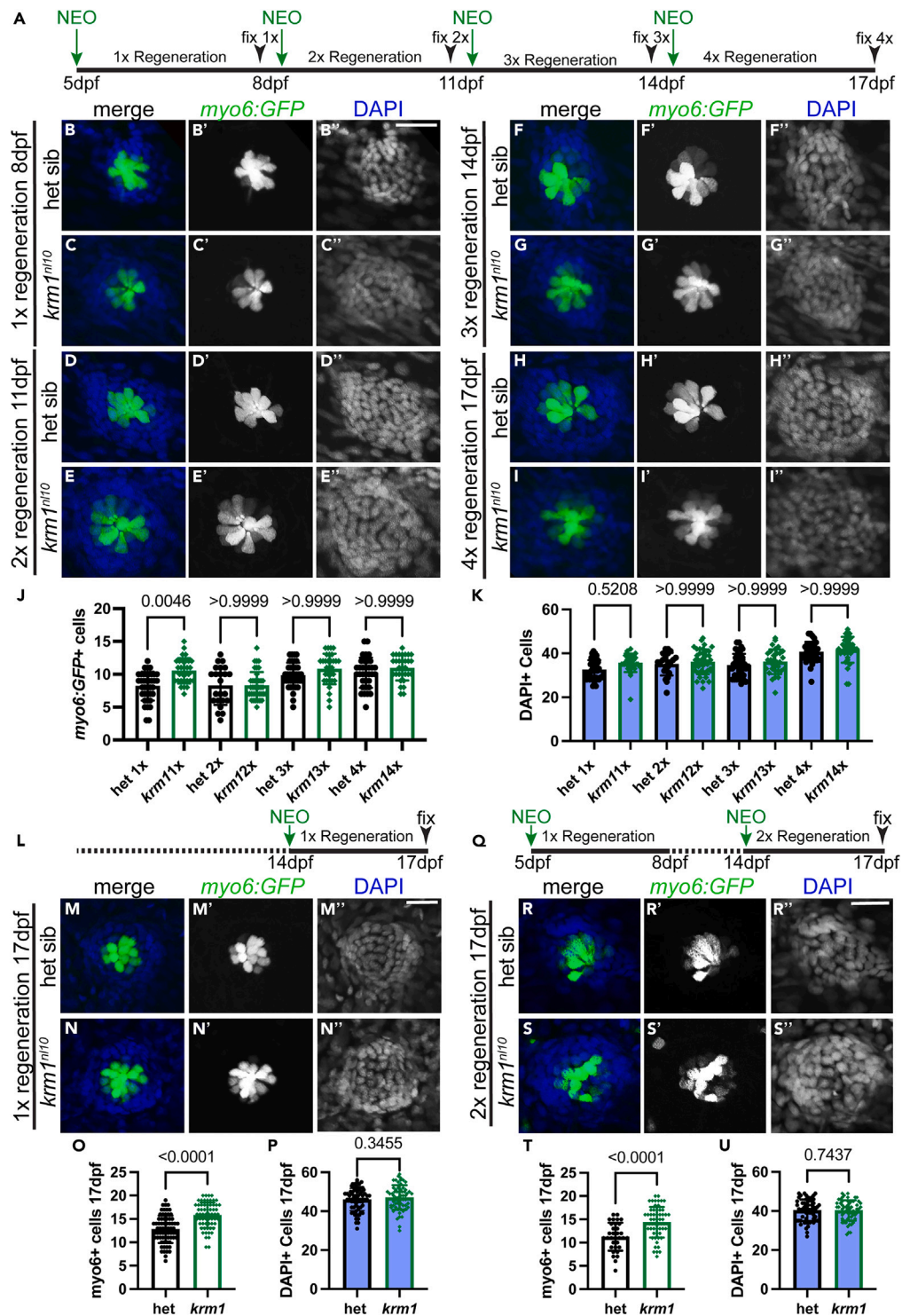
Figure 5. Repeated regeneration eliminates supernumerary hair cells in *krm1*[nl10] larvae

(A) Timeline of *NEO* exposure and repeated regeneration.

(B–I") Confocal projections of NMs expressing *Tg(myosin6b:GFP)*[w186] in hair cells (green) and DAPI-labeling in nuclei following repeated exposures to *NEO* in heterozygous sibling and *krm1*[nl10] mutant NMs at 8dpf following 1 round of *NEO* exposure and regeneration, at 11dpf following 2 rounds of *NEO* exposure and regeneration, at 14dpf following 3 rounds of *NEO* exposure and regeneration, and at 17dpf following 4 rounds of *NEO* exposure and regeneration.

Figure 5. *Continued*

(J–K) Quantification of regenerated *Tg(myosin6b:GFP)*^w186 hair cells or DAPI-labeled nuclei in heterozygous sibling and *krm1*^nl10 mutant NMs at 8dpf, 11dpf, 14dpf, and 17dpf. 8dpf heterozygous sibling n = 38 NM (8 fish) and *krm1*^nl10 mutant n = 30 NM (10 fish), 11dpf heterozygous sibling n = 23 (9 fish) and *krm1*^nl10 n = 39 NM (10 fish), 14dpf heterozygous sibling n = 37 NM (9 fish) and *krm1*^nl10 n = 31 NM (9 fish), and 17dpf heterozygous sibling n = 34 NM (10 fish) and *krm1*^nl10 n = 31 NM (9 fish).

(L) Timeline of a single round NEO-exposure and regeneration between 14 and 17dpf.

(M–N″) Heterozygous sibling and *krm1*^nl10 mutant NMs at 17dpf following 1 round of *NEO* exposure and regeneration.

(O–P) Quantification of regenerated *Tg(myosin6b:GFP)*^w186 hair cells and DAPI-positive cells at 17dpf. Heterozygous siblings n = 68 NM (12 fish) and *krm1*^nl10 n = 62 NM (12 fish). (Q) Timeline of 2 rounds of *NEO* exposure (at 5dpf and 14dpf) and regeneration until 17dpf.

(R–S″) Heterozygous sibling and *krm1*^nl10 mutant NMs at 17dpf following 2x rounds of *NEO* exposure and regeneration.

(T–U) Quantification of regenerated *Tg(myosin6b:GFP)*^w186 hair cells and DAPI-positive cells at 17dpf. Heterozygous siblings n = 33 NM (8 fish) and *krm1*^nl10 n = 58 NM (9 fish). All data presented as mean ± SD, Kruskal-Wallis test, Dunn's multiple comparisons test. Scale bar = 20 μm.

Notch inhibition alters cell numbers in *krm1*^nl10 NMs

The Notch pathway is critical for regulating hair cell regeneration, as manipulation of Notch signaling greatly alters the number of hair cells regenerated following damage.[16,19,22,24] Specifically, Notch signaling regulates proliferation of NM support cells; inhibition of the Notch pathway results in increased support cell proliferation, while activating Notch signaling decreased proliferation.[16,24] As we do not see a significant change in proliferation during regeneration in our *krm1*^nl10 mutant line, we reasoned the Notch pathway might be more important for regenerative NM cell proliferation as compared to Wnt signaling. To test this, we exposed 5dpf heterozygous sibling and *krm1*^nl10 mutant larvae to DMSO or the γ-secretase inhibitor LY441575 for 5 h, ablated hair cells with *NEO*, returned the larvae to DMSO or LY441575 that included BrdU for 24 h, and incubated larvae for an additional 2 days in DMSO or LY441575 alone (Figure 8A). We found BrdU incorporation significantly increased in both heterozygous sibling (Figures 8D–8D‴ and 8G) and *krm1*^nl10 NMs (Figures 8E–8E‴ and 8G) treated with LY441575 relative to DMSO treated larvae (Figures 8A–8C‴ and 8G). As a proportion of total cell number in NMs, BrdU+ cells display a significant increase in the percentage of BrdU+ cells in *krm1*^nl10 mutants treated with LY441575 during regeneration compared with DMSO conditions (Figures 8H and 8I). Additionally, we examined total hair cell numbers and the proportion of regenerated hair cells which incorporated BrdU following Notch inhibition and found a significant increase in both heterozygous and *krm1*^nl10 mutant larvae (Figures 8F and 8J) as compared to DMSO conditions. The results suggest that while overactivating Wnt signaling in *krm1*^nl10 mutants biases a poised population of support cells to give rise to supernumerary hair cells, inhibition of the Notch pathway leads to an increase in proliferation, resulting to a further increase in the number of regenerated hair cells.

Previous work demonstrated both the dorsoventral and anterior-posterior populations of support cells increase in number when the Notch pathway is inhibited during regeneration.[19] We used WISH to demonstrate the Notch pathways members *notch1a, notch3, deltaA*, and *deltaD*, as well as the hair cell progenitor marker *atoh1a*, are expressed at similar levels in heterozygous sibling and *krm1*^nl10 mutant prior to NEO-exposure at 5dpf and 1 day post hair cell ablation (Figures S3A–S3T). Because the Notch pathway regulates the regeneration of both hair cells and dorsoventral support cells, we assessed what happens to these cell populations in *krm1*^nl10 mutant larvae when Notch signaling was conditionally inhibited during regeneration. To further examine the role of dorsoventral support cells during regeneration, we exposed heterozygous or *krm1*^nl10 mutant larvae carrying the *Tg(sost:nlsEos)*^w215 and *Tg(myosin6b:GFP)*^w186 transgenes to DMSO or LY441575. At 5dpf, we incubated the larvae in DMSO or inhibitor for 5 h prior to photoconversion with a UV light and exposure to *NEO* to ablate hair cells, the larvae were then allowed to recover for 3 days and imaged live at 8dpf (Figure 9A). In agreement with our previous experiments, we found
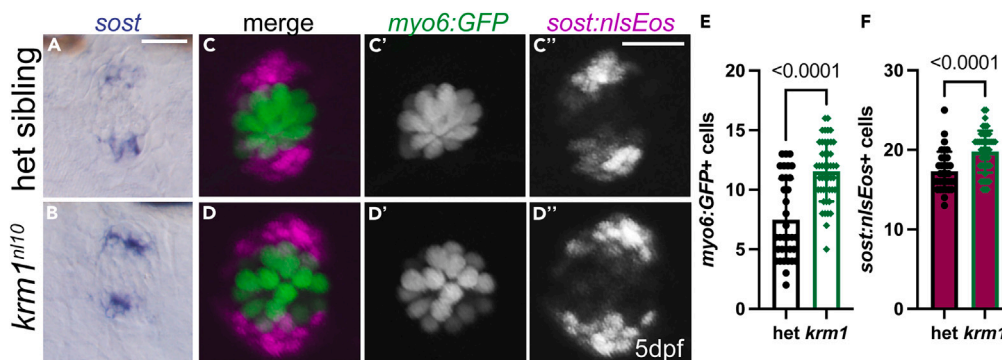

Figure 6. Dorsoventral support cells are increased in *krm1*^nl10 mutant NMs

(A and B) RNA *in situ* hybridization showing *sost* expression in dorsoventral cells in heterozygous sibling and *krm1*^nl10 NMs at 5dpf.

(C–D″) Confocal projections of *Tg(myosin6b:GFP)*^w186 labeled hair cells (green) and *Tg(sost:nlsEos)*^w215 labeled dorsoventral support cells (magenta) immediately following photoconversion in live 5dpf heterozygous sibling and *krm1*^nl10 mutant NMs.

(E–F) Quantification of *Tg(myosin6b:GFP)*^w186 hair cells and total *Tg(sost:nlsEos)*^w215 expressing NM cells. Heterozygous siblings n = 34 NM (8 fish) and *krm1*^nl10 n = 46 NM (9 fish). All data presented as mean ± SD, Mann-Whitney test. Scale bar = 20 μm. See also Figure S2.
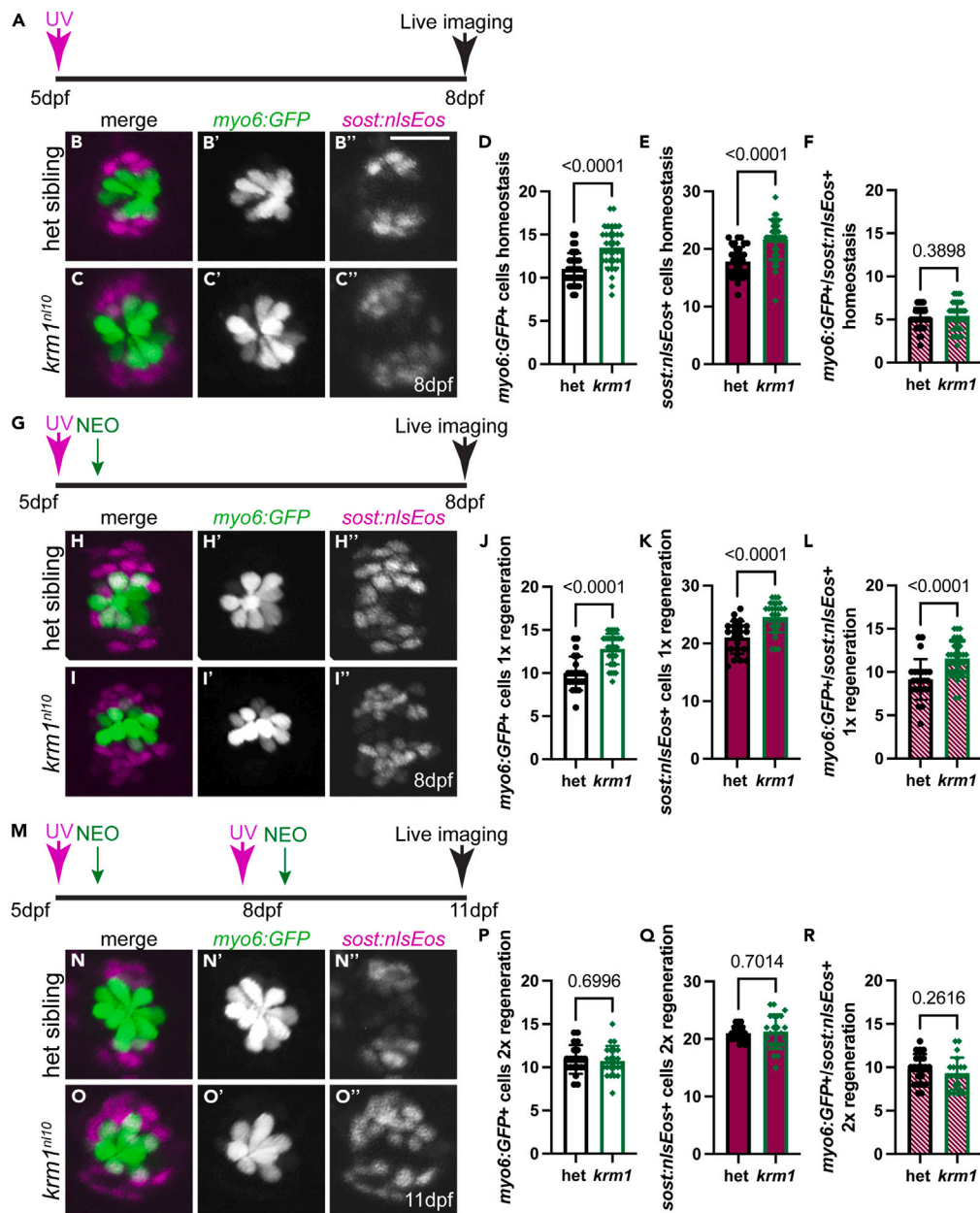
Figure 7. Dorsoventral support cells contribute to supernumerary hair cells following regeneration in *krm1^nl10* mutant NMs

(A) Timeline for *Tg(sost:nlsEos)^w215* photoconversion at 5dpf and homeostatic development until 8dpf.

(B–C″) Homeostasis at 8 days of *Tg(myosin6b:GFP)^w186* labeled hair cells (green) and *Tg(sost:nlsEos)^w215* labeled dorsoventral support cells (magenta) following photoconversion in 5dpf heterozygous sibling and *krm1^nl10* mutant NMs.

(D–F) Quantification of *Tg(myosin6b:GFP)^w186* hair cells, total *Tg(sost:nlsEos)^w215* expressing NM cells, and hair cells expressing both *Tg(myosin6b:GFP)^w186* and *Tg(sost:nlsEos)^w215* at 8dpf. Heterozygous siblings n = 21 NM (12 fish) and *krm1^nl10* n = 22 NM (12 fish).

(G) Timeline for *Tg(sost:nlsEos)^w215* photoconversion and *NEO* at 5dpf and 1 round of regeneration until 8dpf.

(H–I″) 1 round of regeneration of *Tg(myosin6b:GFP)^w186* labeled hair cells (green) and *Tg(sost:nlsEos)^w215* labeled dorsoventral support cells (magenta) following photoconversion at 5dpf and NEO-exposure in heterozygous sibling and *krm1^nl10* mutant NMs.

(J–L) Quantification of *Tg(myosin6b:GFP)^w186* hair cells, total *Tg(sost:nlsEos)^w215* expressing NM cells, and hair cells expressing both *Tg(myosin6b:GFP)^w186* and *Tg(sost:nlsEos)^w215* at 8dpf following 1 round of regeneration. Heterozygous siblings n = 23 NM (8 fish) and *krm1^nl10* n = 31 NM (8 fish).

(M) Timeline for *Tg(sost:nlsEos)^w215* photoconversion and *NEO* at 5dpf and again at 8dpf, for 2 rounds of regeneration until 11dpf.

Figure 7. Continued

(N–O″) 2 rounds of regeneration of *Tg(myosin6b:GFP)*[w186] labeled hair cells (green) and *Tg(sost:nlsEos)*[w215] labeled dorsoventral support cells (magenta) following photoconversion and NEO-exposure at 5dpf and 8dpf in heterozygous sibling and *krm1*[nl10] mutant NMs.

(P–R) Quantification of *Tg(myosin6b:GFP)*[w186] hair cells, total *Tg(sost:nlsEos)*[w215] expressing NM cells, and hair cells expressing both *Tg(myosin6b:GFP)*[w186] and *Tg(sost:nlsEos)*[w215] at 8dpf following 2 rounds of regeneration. Heterozygous siblings n = 21 NM (8 fish) and *krm1*[nl10] n = 22 NM (7 fish). All data presented as mean ± SD, Mann-Whitney test. Scale bar = 20 μm.

krm1[nl10] mutant larvae exposed to DMSO showed a significant increase in the number of regenerated hair cells and dorsoventral *sost:nlsEos*+ support cells (Figures 9C–C″,9F and 9G) as compared to heterozygous sibling controls (Figures 9B–9B″, 9F, and 9G). In comparison to DMSO conditions, LY441575 treatment resulted in a significant increase in the regenerated hair cells in both heterozygous (Figures 9D–D″, 9F, and 9G) and *krm1*[nl10] mutant NMs (Figures 9E–E″, 9F, and 9G), eliminating the difference in populations we see in previous experiments (Figures 9F and 9G). However, when we examined *sost:nlsEos*+ cells in larvae exposed to LY441575, we found a significant increase in heterozygous NMs as compared to DMSO conditions (Figures 9B″, 9D″, 9F, and 9G), but not in *krm1*[nl10] mutant larvae (Figures 9C″, 9E″, 9F, and 9G). These results suggest that the supernumerary *sost:nlsEos* cells in *krm1*[nl10] mutant NMs arise through mechanisms controlled by Wnt signaling rather than the Notch pathway.

As inhibition of Notch signaling increases proliferation, dorsoventral support cell numbers, and hair cell regeneration in *krm1*[nl10] mutant larvae, we next asked if this increase was sufficient to overcome the depletion of poised support cells, we found following multiple rounds of regeneration in mutant NMs. We performed two successive rounds of regeneration between 5dpf and 11dpf using heterozygous sibling and *krm1*[nl10] *myo6:GFP/sost:nlsEos* expressing larvae with continuous exposure to DMSO or LY441575 (Figure 9H). We found in our DMSO treated conditions 2 rounds of regeneration was sufficient to eliminate supernumerary *sost:nlsEos*+ support cells and *myo6:GFP*+ hair cells in *krm1*[nl10] mutant larvae as compared to heterozygous controls (Figures 9I–9J″, 9M, and 9N). In contrast, inhibition of Notch signaling resulted in a significant increase in both *sost:nlsEos*+ and *myo6:GFP*+ cells in heterozygous sibling and *krm1*[nl10] mutant NMs following successive rounds of *NEO* exposure (Figures 9K–L″, 9M, and 9N). Together these results suggest that the Notch pathway regulates support cell proliferation and hair cell regeneration through mechanisms distinct from those regulated by the Wnt pathway and Kremen1 function.

DISCUSSION

Our work demonstrates Krm1 functions in the zebrafish posterior lateral line to regulate the number of dorsoventral support cells and hair cells during NM development and regeneration. Under most conditions Krm1 acts to inhibit canonical Wnt signaling, and the results reported here agree with this function in the lateral line.[29,31] Surprisingly, we found, in contrast to previous analysis of Wnt signaling in the lateral line, regeneration of supernumerary hair cells in *krm1*[nl10] mutants occurs through the direct differentiation of support cells without an increase in proliferation.[13,16,24–27,39,41,42]

Our analysis of Krm1 function during regeneration in the zebrafish posterior lateral line revealed a population of support cells poised to give rise to new hair cells even in the absence of cellular proliferation. These support cells are members of the *sost:nlsEos* expressing dorsoventral population previously demonstrated to be the primary source of regenerating hair cells following neomycin induced damage.[19] As Krm1 functions to inhibit the canonical Wnt pathway, our results examining the loss of Krm1 function suggest Wnt signaling acts to regulate the number of poised progenitor cells. We find repeated ablation of hair cells and successive rounds of regeneration depletes the poised support cells and eliminates supernumerary hair cells in *krm1*[nl10] mutants.

Specific function of support cell populations during lateral line regeneration

Recent studies have begun to identify subsets of support cells with distinct genetic profiles within the zebrafish lateral line which seem to play specific roles during regeneration.[15,16,19,20] Within the specialized subsets of support cells are additional subpopulations that primarily contribute to self-renewal and others that will give rise to regenerating hair cells. Although *krm1* is expressed throughout the NM, loss of Krm1 function seems to particularly result in an increase in the dorsoventral population of *sost:nlsEos*+ support cells and mature hair cells. Within the dorsoventral support cells, there seems to be a further specialized population of cells capable of differentiation into hair cells without first undergoing proliferation. As we find an increase in *sost:nlsEos* support cells in *krm1*[nl10] mutants, Wnt signaling seems to play a role in the regulation of at least a subpopulation of dorsoventral support cells. With the development of more precise expression profiles of cells participating in NM regeneration, we will hopefully be able to specifically determine the identity of the poised support cells.

Wnt and notch signaling in the lateral line

Previous studies demonstrated members of the Wnt pathway are expressed at low levels in the dorsal-ventral poles of NMs during homeostasis and strongly upregulated beginning at 3 h post hair cell ablation with neomycin.[15,16,19,24] Several studies used pharmacological manipulation of the Wnt pathway to dissect the function during regeneration of the zebrafish lateral line.[16,24,25,42,43] These studies, as well as our work, suggest altering Wnt activity specifically results in changes in support cell proliferation; activating Wnt with LiCl, BIO or AZK results in increased proliferation and inhibition of Wnt signaling with IWR-1 leads to decreased support cell proliferation (Figure S1).[16,24,25,42,43] With this history, we were surprised *krm1*[nl10] mutants did not have an increase in proliferation in during regeneration and, in fact, had a decrease in the proportion of BrdU-positive support cells during regeneration (Figure 4).
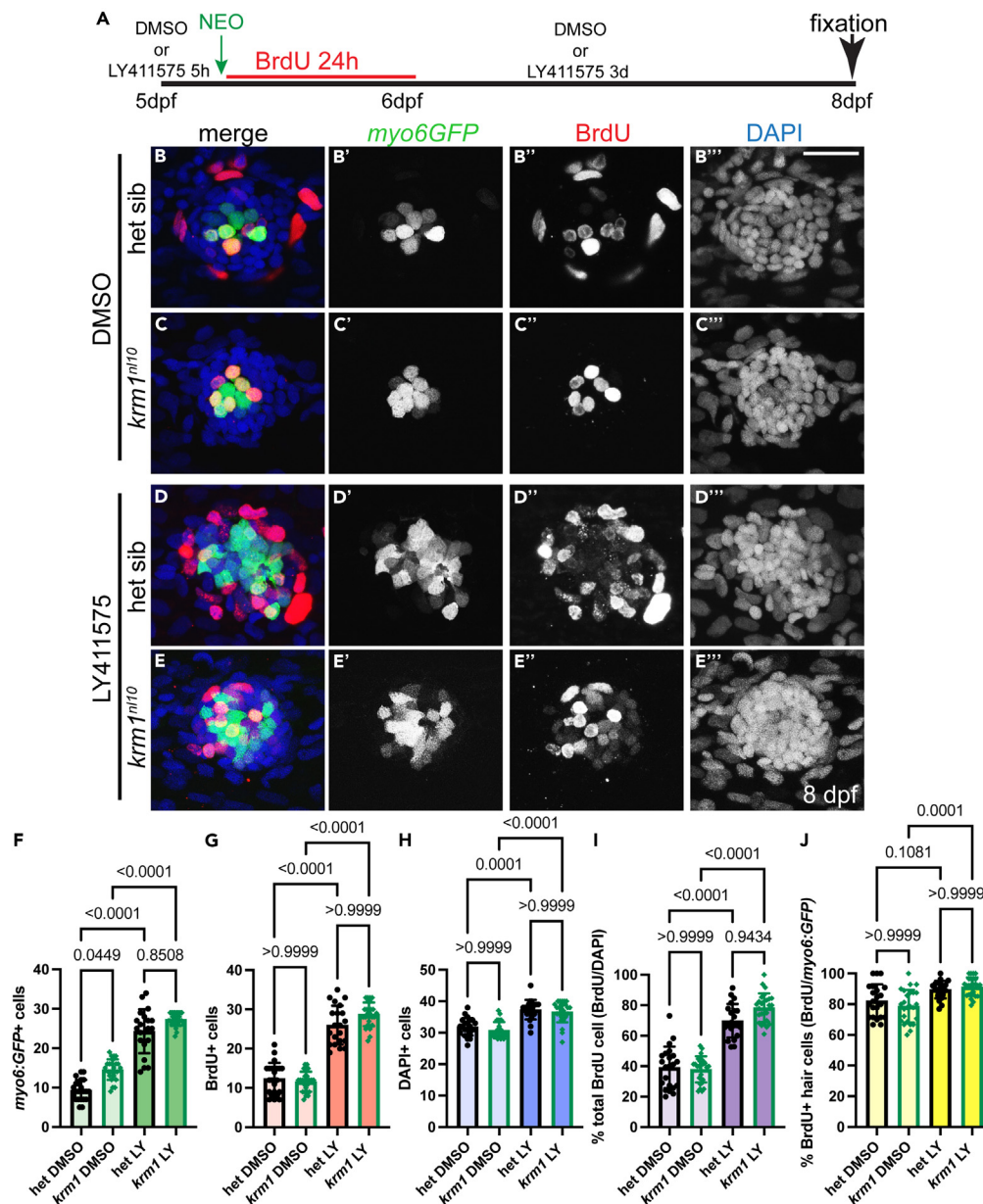
Figure 8. Notch signaling regulates cellular proliferation during regeneration in *krm1^{nl10}* neuromasts

(A) Timeline of drug exposure between 5-8dpf. DMSO or LY411575 at 5dpf for 5-h prior to *NEO* exposure, *NEO* exposure, BrdU incubation for 24 h h in the presence of DMSO or LY411575, and then regeneration to 8dpf with exposure to DMSO or LY411575.

(B–E‴) Confocal projections of L2 neuromasts at 8dpf expressing *Tg(myosin6b:GFP)^{w186}* to label regenerated hair cells (myo6:GFP green), BrdU incorporation (red), and DAPI labeling of nuclei (blue) in heterozygous sibling and *krm1^{nl10}* mutant larvae following exposure to DMSO or LY411575.

(F–J) Quantification of *myo6:GFP*-labeled hair cells at 8dpf following regeneration during exposure to DMSO or LY411575, BrdU-labeled NM cells 8dpf following regeneration during exposure to DMSO or LY411575, percentage of BrdU-positive cells/DAPI-labeled nuclei in NMs, and percentage of *myo6:GFP*-labeled hair cell co-labeled with BrdU. DMSO-exposed heterozygous siblings n = 22 NM (9 fish) and *krm1^{nl10}* n = 26 NM (9 fish); LY411575-exposed heterozygous siblings n = 20 NM (11 fish) and *krm1^{nl10}* n = 26 NM (9 fish). All data presented as mean ± SD, Kruskal-Wallis test, Dunn's multiple comparisons test. Scale bar = 20 μm. See also Figure S3.

The difference between previous pharmacological manipulation experiments and the *krm1^{nl10}* mutants might be a result of the specificity of the targets affected. AZK and BIO both activate the Wnt pathway though inhibition of glycogen synthase kinase 3β (GSK3β) and disruption of the destruction complex, releasing β-catenin and allowing Wnt-mediated gene transcription.[38] While GSK3β is strongly associated with canonical Wnt signaling, regulation of cell behaviors via multiple pathways also integrate GSK3beta activity, in particular
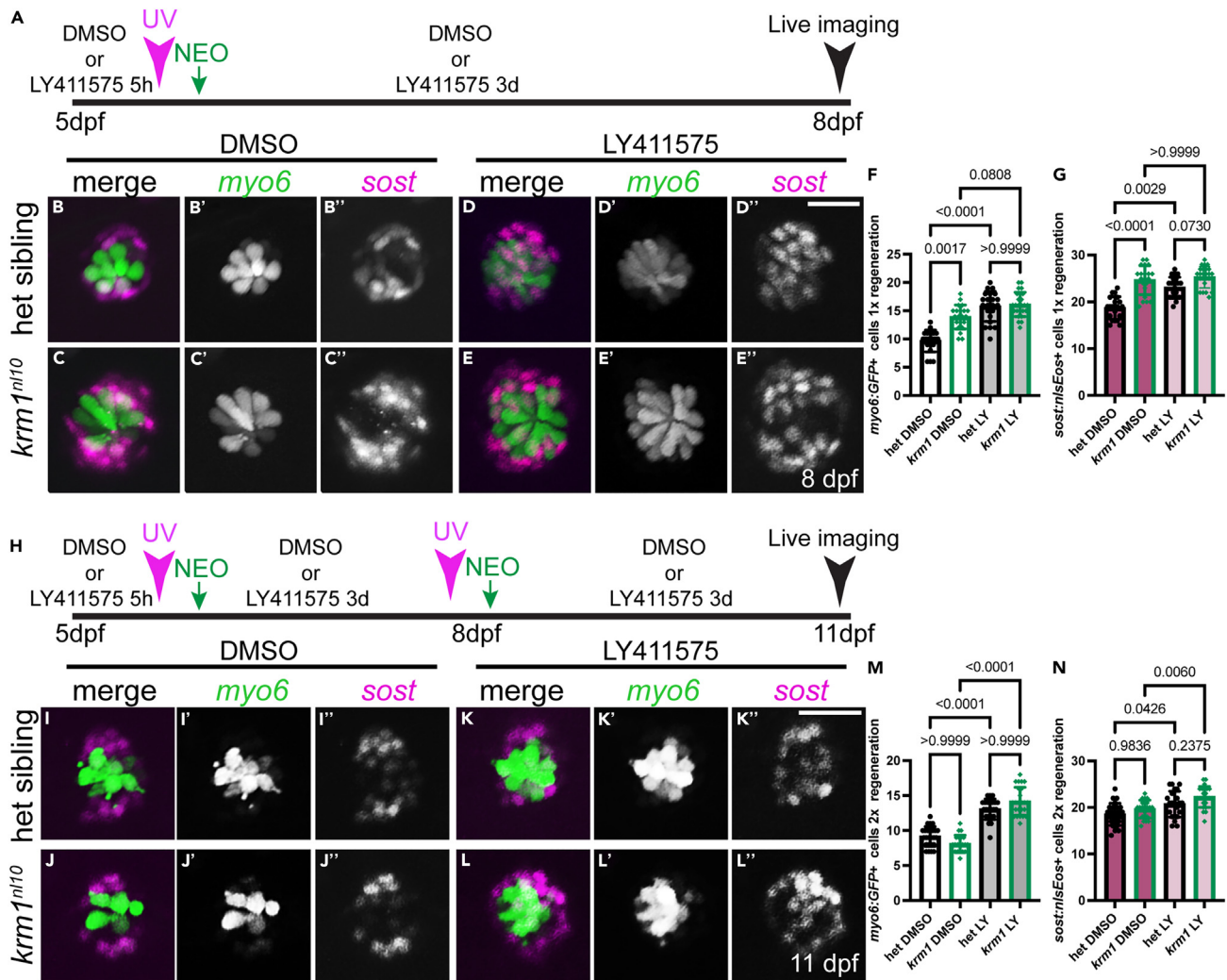
Figure 9. Notch signaling alters NM cell numbers following repeated damage

(A) Timeline of drug exposure from 5-8dpf, photoconversion, *NEO* exposure, regeneration, and live imaging.

(B–E'') Live confocal projections of *Tg(myosin6b:GFP)^w186* labeled cells (*myo6*, green) and *Tg(sost:nlsEos)^w215* labeled cells (*sost*, magenta) in larvae exposed to DMSO or LY411575 and 1 round of regeneration in heterozygous sibling *krm1^nl10* mutant larvae.

(F–G) Quantification of *Tg(myosin6b:GFP)^w186* labeled hair cells and *Tg(sost:nlsEos)^w215* labeled cells at 8dpf following regeneration during exposure to DMSO or LY411575. DMSO-exposed heterozygous siblings n = 20 NM (9 fish) and *krm1^nl10* n = 21 NM (9 fish); LY411575-exposed heterozygous siblings n = 22 NM (9 fish) and *krm1^nl10* n = 25 NM (11 fish).

(H) Timeline for drug exposure, *Tg(sost:nlsEos)^w215* photoconversion and *NEO* at 5dpf and again at 8dpf, for 2 rounds of regeneration until 11dpf.

(I–L'') Heterozygous sibling and *krm1^nl10* mutant larvae exposed to DMSO or LY411575 during 2 rounds of regeneration.

(M and N) Quantification of *Tg(myosin6b:GFP)^w186* labeled cells and *Tg(sost:nlsEos)^w215* labeled cells following 2 rounds of regeneration in the presence of DMSO or LY411575. DMSO-exposed heterozygous siblings n = 24 NM (11 fish) and *krm1^nl10* n = 23 NM (10 fish); LY411575-exposed heterozygous siblings n = 22 NM (8 fish) and *krm1^nl10* n = 24 NM (10 fish). All data presented as mean ± SD, Kruskal-Wallis test, Dunn's multiple comparisons test. Scale bar = 20 μm. See also Figure S3.

through the AKT/mTOR pathway to promote proliferation and regeneration.[44] Along similar lines, IWR-1 inhibits Tankyrase, which results in the stabilization of Axin and the increased phosphorylation and subsequent degradation of β-catenin. Tankyrase plays roles in many signaling pathways that can impinge on cellular proliferation.[45] Thus, the changes in proliferation seen during regeneration with exposure to pharmacological manipulations may be the result of alterations in multiple pathways and not limited to canonical Wnt signaling.

The Notch/Delta pathway is critical for regulating cellular behavior during development and regeneration in the lateral line.[16,19,22,24,27] Inhibition of Notch signaling results in dramatic increases in proliferation, support cell numbers, and hair cell formation.[16,22,24] Previous work examining the results of simultaneously manipulating the Notch and Wnt pathways using pharmacological methods specifically resulted

in changes in the levels of proliferation during lateral line regeneration.[16,24] In contrast, our experiments assessing regeneration using the *krm1^{nl10}* mutant line, suggest overactivating Wnt signaling increases hair cell progenitor specification and differentiation without altering overall levels of proliferation. However, additionally inhibiting Notch signaling in our *krm1^{nl10}* mutants during regeneration resulted in increases in proliferation and additional increases hair cell differentiation. These results suggest the Notch and Wnt pathways might regulate independent mechanisms controlling lateral line regeneration. Future work examining additional Wnt pathway mutants should provide a more detailed understanding of the role of Wnt signaling in regulating regeneration.

Krm1 and human hearing

Recent studies using mammalian inner ear cell cultures suggest manipulating the Notch and Wnt pathways are critical to regrowing damaged hair cells.[46,47] Interestingly, while there are conflicting results for upregulation and downregulation of Notch signaling as a mechanism to promote regeneration, upregulation of Wnt signaling is consistently necessary.[46,47] Krm1 is expressed in the support cells of the mammalian cochlea, making it a potential target for therapeutic intervention: inhibition of Krm1 function might be required for support cells to re-enter a more progenitor-like stage to then differentiate as mechanosensory hair cells to restore hearing. Future work will be needed to determine if regulation of Krm1 function also plays a role in hair regeneration in the inner ear.

Limitations of the study

In this study, we used the *krm1^{nl10}* mutant zebrafish line to determine if Krm1 function regulates hair cell regeneration. We determined that *krm1^{nl10}* mutants form more dorsoventral support cells in their neuromasts as compared to controls, and that these cells can regenerate supernumerary hair cells in the absence of increase proliferation. One of the primary limitations of this study is that we do not know the precise identity of these poised dorsoventral cells. Future studies examining existing gene expression profiles of the lateral line or single-cell RNA sequencing of *krm1^{nl10}* mutants, will help identify this poised progenitor population. Another limitation is that the current study does not address the role of these poised progenitor cells in wild-type fish under homeostatic conditions. It is possible that this is a small population of support cells, which can rapidly replenish hair cells damaged during the normal life cycle of the fish. Future work is needed to address these questions.

STAR★METHODS

Detailed methods are provided in the online version of this paper and include the following:

- KEY RESOURCES TABLE
- RESOURCE AVAILABILITY
  - ○ Lead contact
  - ○ Material availability
  - ○ Data and code availability
- EXPERIMENTAL MODEL
  - ○ Zebrafish lines and maintenance
- METHOD DETAILS
  - ○ Whole mount RNA *in situ* hybridization
  - ○ HCR fluorescent RNA *in situ* hybridization
  - ○ Immunohistochemistry and FM1-43FX labeling
  - ○ Neomycin exposure and regeneration
  - ○ BrdU incorporation
  - ○ Inhibitor treatment conditions
  - ○ Photoconversion
  - ○ Image collection
- QUANTIFICATION AND STATISTICAL ANALYSIS

SUPPLEMENTAL INFORMATION

Supplemental information can be found online at https://doi.org/10.1016/j.isci.2023.108678.

AUTHOR CONTRIBUTIONS

Conceptualization & Methodology, E.M., M.K., J.B., and H.F.M.; Investigation: E.M., M.K., B.L., J.B., and H.F.M.; Writing – Original Draft, H.F.M; Writing – Review and Editing, J.B., H.F.M., and J.S.; Funding Acquisition, H.F.M.

DECLARATION OF INTERESTS

The authors declare no competing interests.

REFERENCES

1. Frisina, R.D., Wheeler, H.E., Fossa, S.D., Kerns, S.L., Fung, C., Sesso, H.D., Monahan, P.O., Feldman, D.R., Hamilton, R., Vaughn, D.J., et al. (2016). Comprehensive Audiometric Analysis of Hearing Impairment and Tinnitus After Cisplatin-Based Chemotherapy in Survivors of Adult-Onset Cancer. J. Clin. Oncol. *34*, 2712–2720.

2. Goderis, J., De Leenheer, E., Smets, K., Van Hoecke, H., Keymeulen, A., and Dhooge, I. (2014). Hearing loss and congenital CMV infection: a systematic review. Pediatrics *134*, 972–982.

3. Honeybrook, A., Patki, A., Chapurin, N., and Woodard, C. (2017). Hearing and Mortality Outcomes following Temporal Bone Fractures. Craniomaxillofac. Trauma Reconstr. *10*, 281–285.

4. Lie, A., Skogstad, M., Johnsen, T.S., Engdahl, B., and Tambs, K. (2016). Noise-induced hearing loss in a longitudinal study of Norwegian railway workers. BMJ Open *6*, e011923.

5. Xu, S., and Yang, N. (2021). Research Progress on the Mechanism of Cochlear Hair Cell Regeneration. Front. Cell. Neurosci. *15*, 732507.

6. Cruz, I.A., Kappedal, R., Mackenzie, S.M., Hailey, D.W., Hoffman, T.L., Schilling, T.F., and Raible, D.W. (2015). Robust regeneration of adult zebrafish lateral line hair cells reflects continued precursor pool maintenance. Dev. Biol. *402*, 229–238.

7. Pinto-Teixeira, F., Viader-Llargués, O., Torres-Mejía, E., Turan, M., González-Gualda, E., Pola-Morell, L., and López-Schier, H. (2015). Inexhaustible hair-cell regeneration in young and aged zebrafish. Biol. Open *4*, 903–909.

8. Brignull, H.R., Raible, D.W., and Stone, J.S. (2009). Feathers and fins: non-mammalian models for hair cell regeneration. Brain Res. *1277*, 12–23.

9. Pickett, S.B., and Raible, D.W. (2019). Water Waves to Sound Waves: Using Zebrafish to Explore Hair Cell Biology. J. Assoc. Res. Otolaryngol. *20*, 1–19.

10. Nicolson, T. (2017). The genetics of hair-cell function in zebrafish. J. Neurogenet. *31*, 102–112.

11. Denans, N., Baek, S., and Piotrowski, T. (2019). Comparing Sensory Organs to Define the Path for Hair Cell Regeneration. Annu. Rev. Cell Dev. Biol. *35*, 567–589.

12. Monroe, J.D., Rajadinakaran, G., and Smith, M.E. (2015). Sensory hair cell death and regeneration in fishes. Front. Cell. Neurosci. *9*, 131.

13. Kniss, J.S., Jiang, L., and Piotrowski, T. (2016). Insights into sensory hair cell regeneration from the zebrafish lateral line. Curr. Opin. Genet. Dev. *40*, 32–40.

14. Thomas, A.J., Wu, P., Raible, D.W., Rubel, E.W., Simon, J.A., and Ou, H.C. (2015). Identification of small molecule inhibitors of cisplatin-induced hair cell death: results of a 10,000 compound screen in the zebrafish lateral line. Otol. Neurotol. *36*, 519–525.

15. Baek, S., Tran, N.T.T., Diaz, D.C., Tsai, Y.Y., Acedo, J.N., Lush, M.E., and Piotrowski, T. (2022). Single-cell transcriptome analysis reveals three sequential phases of gene expression during zebrafish sensory hair cell regeneration. Dev. Cell *57*, 799–819.e6.

16. Lush, M.E., Diaz, D.C., Koenecke, N., Baek, S., Boldt, H., St Peter, M.K., Gaitan-Escudero, T., Romero-Carvajal, A., Busch-Nentwich, E.M., Perera, A.G., et al. (2019). scRNA-Seq reveals distinct stem cell populations that drive hair cell regeneration after loss of Fgf and Notch signaling. Elife *8*, e44431.

17. Qian, F., Wei, G., Gao, Y., Wang, X., Gong, J., Guo, C., Wang, X., Zhang, X., Zhao, J., Wang, C., et al. (2022). Single-cell RNA-sequencing of zebrafish hair cells reveals novel genes potentially involved in hearing loss. Cell. Mol. Life Sci. *79*, 385.

18. Shi, T., Beaulieu, M.O., Saunders, L.M., Fabian, P., Trapnell, C., Segil, N., Crump, J.G., and Raible, D.W. (2023). Single-cell transcriptomic profiling of the zebrafish inner ear reveals molecularly distinct hair cell and supporting cell subtypes. Elife *12*, e82978.

19. Thomas, E.D., and Raible, D.W. (2019). Distinct progenitor populations mediate regeneration in the zebrafish lateral line. Elife *8*, e43736.

20. Jimenez, E., Slevin, C.C., Song, W., Chen, Z., Frederickson, S.C., Gildea, D., Wu, W., Elkahloun, A.G., Ovcharenko, I., and Burgess, S.M. (2022). A regulatory network of Sox and Six transcription factors initiate a cell fate transformation during hearing regeneration in adult zebrafish. Cell Genom. *2*, 100170.

21. Akil, O., Hall-Glenn, F., Chang, J., Li, A., Chang, W., Lustig, L.R., Alliston, T., and Hsiao, E.C. (2014). Disrupted bone remodeling leads to cochlear overgrowth and hearing loss in a mouse model of fibrous dysplasia. PLoS One *9*, e94989.

22. Ma, E.Y., Rubel, E.W., and Raible, D.W. (2008). Notch signaling regulates the extent of hair cell regeneration in the zebrafish lateral line. J. Neurosci. *28*, 2261–2273.

23. Mi, X.X., Yan, J., Li, Y., and Shi, J.P. (2019). Wnt/β-catenin signaling was activated in supporting cells during exposure of the zebrafish lateral line to cisplatin. Ann. Anat. *226*, 48–56.

24. Romero-Carvajal, A., Navajas Acedo, J., Jiang, L., Kozlovskaja-Gumbrienė, A., Alexander, R., Li, H., and Piotrowski, T. (2015). Regeneration of Sensory Hair Cells Requires Localized Interactions between the Notch and Wnt Pathways. Dev. Cell *34*, 267–282.

25. Tang, D., He, Y., Li, W., and Li, H. (2019). Wnt/β-catenin interacts with the FGF pathway to promote proliferation and regenerative cell proliferation in the zebrafish lateral line neuromast. Exp. Mol. Med. *51*, 1–16.

26. Tang, D., Lin, Q., He, Y., Chai, R., and Li, H. (2016). Inhibition of H3K9me2 Reduces Hair Cell Regeneration after Hair Cell Loss in the Zebrafish Lateral Line by Down-Regulating the Wnt and Fgf Signaling Pathways. Front. Mol. Neurosci. *9*, 39.

27. Ye, Z., Su, Z., Xie, S., Liu, Y., Wang, Y., Xu, X., Zheng, Y., Zhao, M., and Jiang, L. (2020). Yap-lin28a axis targets let7-Wnt pathway to restore progenitors for initiating regeneration. Elife *9*, e55771.

28. Mao, B., Wu, W., Davidson, G., Marhold, J., Li, M., Mechler, B.M., Delius, H., Hoppe, D., Stannek, P., Walter, C., et al. (2002). Kremen proteins are Dickkopf receptors that regulate Wnt/beta-catenin signalling. Nature *417*, 664–667.

29. Niehrs, C. (2006). Function and biological roles of the Dickkopf family of Wnt modulators. Oncogene *25*, 7469–7481.

30. Mulvaney, J.F., Thompkins, C., Noda, T., Nishimura, K., Sun, W.W., Lin, S.Y., Coffin, A., and Dabdoub, A. (2016). Kremen1 regulates mechanosensory hair cell development in the mammalian cochlea and the zebrafish lateral line. Sci. Rep. *6*, 31668.

31. McGraw, H.F., Culbertson, M.D., and Nechiporuk, A.V. (2014). Kremen1 restricts Dkk activity during posterior lateral line development in zebrafish. Development *141*, 3212–3221.

32. Wada, H., Ghysen, A., Asakawa, K., Abe, G., Ishitani, T., and Kawakami, K. (2013). Wnt/Dkk negative feedback regulates sensory organ size in zebrafish. Curr. Biol. *23*, 1559–1565.

33. Thisse, C., and Thisse, B. (2008). High-resolution in situ hybridization to whole-mount zebrafish embryos. Nat. Protoc. *3*, 59–69.

34. Ibarra-García-Padilla, R., Howard, A.G.A., 4th, Singleton, E.W., and Uribe, R.A. (2021). A protocol for whole-mount immuno-coupled hybridization chain reaction (WICHCR) in zebrafish embryos and larvae. STAR Protoc. *2*, 100709.

35. Schwarzkopf, M., Liu, M.C., Schulte, S.J., Ives, R., Husain, N., Choi, H.M.T., and Pierce, N.A. (2021). Hybridization chain reaction enables a unified approach to multiplexed, quantitative, high-resolution immunohistochemistry and in situ hybridization. Development *148*.

36. Seiler, C., Ben-David, O., Sidi, S., Hendrich, O., Rusch, A., Burnside, B., Avraham, K.B., and Nicolson, T. (2004). Myosin VI is required for structural integrity of the apical surface of sensory hair cells in zebrafish. Dev. Biol. *272*, 328–338.

37. Seiler, C., and Nicolson, T. (1999). Defective calmodulin-dependent rapid apical endocytosis in zebrafish sensory hair cell mutants. J. Neurobiol. *41*, 424–434.

38. Kunick, C., Lauenroth, K., Leost, M., Meijer, L., and Lemcke, T. (2004). 1-Azakenpaullone is a selective inhibitor of glycogen synthase

kinase-3 beta. Bioorg. Med. Chem. Lett. *14*, 413–416.

39. Jacques, B.E., Montgomery, W.H., 4th, Uribe, P.M., Yatteau, A., Asuncion, J.D., Resendiz, G., Matsui, J.I., and Dabdoub, A. (2014). The role of Wnt/beta-catenin signaling in proliferation and regeneration of the developing basilar papilla and lateral line. Dev. Neurobiol. *74*, 438–456.

40. Thomas, E.D., Cruz, I.A., Hailey, D.W., and Raible, D.W. (2015). There and back again: development and regeneration of the zebrafish lateral line system. Wiley Interdiscip. Rev. Dev. Biol. *4*, 1–16.

41. Head, J.R., Gacioch, L., Pennisi, M., and Meyers, J.R. (2013). Activation of canonical Wnt/β-catenin signaling stimulates proliferation in neuromasts in the zebrafish posterior lateral line. Dev. Dyn. *242*, 832–846.

42. Li, R., Liao, G., Yin, G., Wang, B., Yan, M., Lin, X., Zhang, W., Chen, X., Du, S., and Yuan, Y. (2018). Ionizing Radiation Blocks Hair Cell Regeneration in Zebrafish Lateral Line Neuromasts by Preventing Wnt Signaling. Mol. Neurobiol. *55*, 1639–1651.

43. Jacques, B.E., Montgomery, W.H., 4th, Uribe, P.M., Yatteau, A., Asuncion, J.D., Resendiz, G., Matsui, J.I., and Dabdoub, A. (2014). The role of Wnt/β-catenin signaling in proliferation and regeneration of the developing basilar papilla and lateral line. Dev. Neurobiol. *74*, 438–456.

44. Hottin, C., Perron, M., and Roger, J.E. (2022). GSK3 Is a Central Player in Retinal Degenerative Diseases but a Challenging Therapeutic Target. Cells *11*.

45. Kim, M.K. (2018). Novel insight into the function of tankyrase. Oncol. Lett. *16*, 6895–6902.

46. Ueda, Y., Nakamura, T., Nie, J., Solivais, A.J., Hoffman, J.R., Daye, B.J., and Hashino, E. (2023). Defining developmental trajectories of prosensory cells in human inner ear organoids at single-cell resolution. Development *150*, dev201071.

47. Zhang, L., Fang, Y., Tan, F., Guo, F., Zhang, Z., Li, N., Sun, Q., Qi, J., and Chai, R. (2023). AAV-Net1 facilitates the trans-differentiation of supporting cells into hair cells in the murine cochlea. Cell. Mol. Life Sci. *80*, 86.

48. Itoh, M., and Chitnis, A.B. (2001). Expression of proneural and neurogenic genes in the zebrafish lateral line primordium correlates with selection of hair cell fate in neuromasts. Mech. Dev. *102*, 263–266.

49. Schindelin, J., Arganda-Carreras, I., Frise, E., Kaynig, V., Longair, M., Pietzsch, T., Preibisch, S., Rueden, C., Saalfeld, S., Schmid, B., et al. (2012). Fiji: an open-source platform for biological-image analysis. Nat. Methods *9*, 676–682.

50. Haddon, C., Smithers, L., Schneider-Maunoury, S., Coche, T., Henrique, D., and Lewis, J. (1998). Multiple delta genes and lateral inhibition in zebrafish primary neurogenesis. Development *125*, 359–370.

51. Kimmel, C.B., Ballard, W.W., Kimmel, S.R., Ullmann, B., and Schilling, T.F. (1995). Stages of embryonic development of the zebrafish. Dev. Dyn. *203*, 253–310.

52. Kossack, M.E., and Draper, B.W. (2019). Genetic regulation of sex determination and maintenance in zebrafish (Danio rerio). Curr. Top. Dev. Biol. *134*, 119–149.

53. Logel, J., Dill, D., and Leonard, S. (1992). Synthesis of cRNA probes from PCR-generated DNA. Biotechniques *13*, 604–610.

54. Ungos, J.M., Karlstrom, R.O., and Raible, D.W. (2003). Hedgehog signaling is directly required for the development of zebrafish dorsal root ganglia neurons. Development *130*, 5351–5362.

55. Owens, K.N., Santos, F., Roberts, B., Linbo, T., Coffin, A.B., Knisely, A.J., Simon, J.A., Rubel, E.W., and Raible, D.W. (2008). Identification of genetic and chemical modulators of zebrafish mechanosensory hair cell death. PLoS Genet. *4*, e1000020.

56. Harris, J.A., Cheng, A.G., Cunningham, L.L., MacDonald, G., Raible, D.W., and Rubel, E.W. (2003). Neomycin-induced hair cell death and rapid regeneration in the lateral line of zebrafish (Danio rerio). J. Assoc. Res. Otolaryngol. *4*, 219–234.

57. Laguerre, L., Soubiran, F., Ghysen, A., König, N., and Dambly-Chaudière, C. (2005). Cell proliferation in the developing lateral line system of zebrafish embryos. Dev. Dyn. *233*, 466–472.

STAR★METHODS

KEY RESOURCES TABLE

REAGENT or RESOURCE	SOURCE	IDENTIFIER
Antibodies		
Mouse monoclonal anti-Otoferlin antibody	DSHB	Cat# HCS-1; RRID: AB_10804296
Mouse monoclonal anti-BrdU antibody	BD Biosciences	Cat# 347580; RRID: AB_10015219
Rabbit polyclonal anti-Sox2 antibody	Thermo Fisher	Cat# PA5-85144; RRID: AB_2792291
Alexa Fluor 674 goat anti-mouse antibody	Thermo Fisher	Cat# A-21236; RRID: AB_2535805
Alexa Fluor 568 goat anti-mouse antibody	Thermo Fisher	Cat# A-11004; RRID: AB_2534072
Alexa Fluor 674 goat anti-rabbit antibody	Thermo Fisher	Cat# A-21244; RRID: AB_2535812
Anti-Digoxigenin-AP, Fab Fragments	Millipore Sigma	Cat# 11093274910; RRID: AB_2734716
Chemicals, peptides, and recombinant proteins		
DAPI	Thermo Fisher	Cat# D1306
Neomycin sulfate	Millipore Sigma	Cat# N0400000
BrdU (5-Bromo-2′-deoxyuridine)	Millipore Sigma	Cat# 19–160
LY411575	Millipore Sigma	Cat# SML0506
AZK (1-azakenpaullone)	Millipore Sigma	Cat# A3734
IWR-1-endo	Millipore Sigma	Cat# 681669
Digoxygenin RNA labeling mix	Millipore Sigma	Cat# 11277073901
Critical commercial assays		
HCR RNA-FISH Bundle	Molecular Instruments	https://store.molecularinstruments.com/new-bundle/rna-fish
Experimental models: Organisms/strains		
Zebrafish: Wildtype *AB	ZIRC http://zebrafish.org	ZFIN: ZDB-960809-7
Zebrafish: *krm1*[nl10]	(McGraw et al., 2014)[31]	RRID: ZFIN_ZDB-GENO-141113-8
Zebrafish: *Tg(myosin6b:GFP)*[w186]	(Thomas and Raible, 2019)[19]	RRID: ZFIN_ZDB_B-ALT-170321-13
Zebrafish: *Tg(sost:nlsEos)*[w215]	(Thomas and Raible, 2019)[19]	RRID: ZFIN_ZDB-ALT_190909-10
Zebrafish: *Tg(sfrp1a:nlsEos)*[w217]	(Thomas and Raible, 2019)[19]	RRID: ZFIN_ZDB_GENO-200218-3
Oligonucleotides		
atoh1a RNA *in situ* hybridization probe	(Itoh and Chitnis, 2001)[48]	ZFIN: ZDB-GENE-990415-17
notch3 RNA *in situ* hybridization probe	(Itoh and Chitnis, 2001)[48]	ZFIN: ZDB-GENE-000329-5
deltaA RNA *in situ* hybridization probe	(Haddon et al., 1998)[49]	ZFIN: ZDB-GENE-980526-29
deltaD RNA *in situ* hybridization probe	(Haddon et al., 1998)[50]	ZFIN: ZDB-GENE-990415-47
notch1a RNA *in situ* hybridization probe	(Haddon et al., 1998)[50]	ZFIN: ZDB-GENE-990415-173
wnt2 *in situ* hybridization probe template primers Forward:5′TTGGATCGCAAGTGATGTGC3′ Reverse:5′CCAAGCTTCTAATACGACTCACT ATAGGGAGAAAGCCCGTCCCATATTGGTT3	IDT	ZFIN: ZDB-GENE-980526-416
kremen1 *in situ* hybridization probe template primers Forward:5′GCCACAACACCATGTGGACC3′ Reverse:5′CCAAGCTTCTAATACGACTC ACTATAGGGAGATGGGCACCGTGGCATTATTT3′	IDT	ZFIN: ZDB-GENE-070705-262
ctnnb1 *in situ* hybridization probe template primers Forward:5′GATGCTCAAACATGCCGTGG3′ Reverse:5′CCAAGCTTCTAATACGACTCAC TATAGGGAGACATGCCCTCCTGTTTGGTGG3′	IDT	ZFIN: ZDB-GENE-980526-362

(Continued on next page)

Continued

REAGENT or RESOURCE	SOURCE	IDENTIFIER
six1a *in situ* hybridization probe template primers Forward:5′CTCGTTCGGCTTTACGCAAG3′ Reverse:5′CCAAGCTTCTAATACGACTCACT ATAGGGAGAGATCTGATGCGGATGCCCTT3′	IDT	ZFIN: ZDB-GENE-040718-155
tnfsf10L3 *in situ* hybridization probe template primers Forward:5′TCTTTGGAGAGCCGTGCATT3′ Reverse:5′CCAAGCTTCTAATACGACTCACTA TAGGGAGACTCACTGTCCGGAGACCAAC3′	IDT	ZFIN: ZDB-GENE-070606-1
sost *in situ* hybridization probe template primers Forward:5′ACGGACCAAACCGGACATAC3′ Reverse:5′CCAAGCTTCTAATACGACTCACTAT AGGGAGAATGAACCGCTTGAGCAGGAA3′	IDT	ZFIN: ZDB-GENE-110411-139
sfrp1a *in situ* hybridization probe template primers Forward:5′ATAAGAACTGCGACCCAGGC3′ Reverse:5′CCAAGCTTCTAATACGACTCACT ATAGGGAGACCACCTTGCGTCCCATGATA3′	IDT	ZFIN: ZDB-GENE-040310-5
lfng *in situ* hybridization probe template primers Forward:5′CACCTGTCTGGGGTTTCTGT3′ Reverse:5′CCAAGCTTCTAATACGACTCACT ATAGGGAGATCTGTCGCATGTTTCTGGAG3′	IDT	ZFIN: ZDB-GENE-980605-16
isl1a *in situ* hybridization probe template primers Forward:5′CAACATCGGTTTCAGCAAGA3′ Reverse:5′CCAAGCTTCTAATACGACTCACT ATAGGGAGAAGGCTGGTCGATGTCACTCT3′	IDT	ZFIN: ZDB-GENE-980526-112
tnfsf10L3 RNA FISH Probe	Molecular Instruments	GenBank: NM_001042713.1
krm1 RNA FISH Probe	Molecular Instruments	GenBank: NM_001114917.1
Software and algorithms		
FIJI	(Schindelin et al., 2012)[49]	https://imagej.nih.gov/ij/
PRISM	GraphPad	https://www.graphpad.com
Deposited data		
Raw data files	This paper	Mendeley Database: https://data.mendeley.com/datasets/hg3y4v2cbf/1

RESOURCE AVAILABILITY

Lead contact

Further information and requests for resources, zebrafish or other materials should be directed to and will be fulfilled by the lead contact, Hillary F. McGraw (mcgrawh@umkc.edu).

Material availability

All materials are available upon e-mail request to the lead contact, Hillary F. McGraw (mcgrawh@umkc.edu).

Data and code availability

Raw data files are available at Mendeley Data (https://data.mendeley.com/datasets/hg3y4v2cbf/1). No code was generated in this study.

EXPERIMENTAL MODEL

Zebrafish lines and maintenance

The following zebrafish lines were used: wild-type*AB (ZIRC; http://zebrafish.org), *Tg(myosin6b:GFP)*[w186],[19] *Tg(sost:nlsEos)*[w215],[19] *Tg(sfpr1a:nlsEos)*[w217],[19] and *krm1*[nl10].[31] Zebrafish were maintained and staged according to standard protocols.[51] This study used larvae at stages between 5 and 17dpf. Control animals were either wild-type or *krm1*[nl10] heterozygous age matched larvae. *krm1*[nl10] homozygous

mutants were identified by their characteristic posterior lateral line truncation.[31] Larvae were kept in E3 embryo medium (14.97 mM NaCl, 500 μM KCl, 42 μM Na_2HPO_4, 150 μM KH_2PO_4, 1 mM $CaCl_2$ dihydrate, 1 mM $MgSO_4$, 0.714 mM $NaHCO_3$, pH 7.2). For all experiments, larvae were treated with tricaine (Syndel) prior to fixation in 4% paraformaldehyde/PBS (Thermo Fisher). All work was performed in accordance with the McGraw laboratory protocol #41153 approved by the UMKC IACUC committee. In laboratory zebrafish lines, sexual determination and differentiation occurs at ~25dpf ([52]), after the timepoints used in this study.

METHOD DETAILS

Whole mount RNA *in situ* hybridization

Whole mount RNA *in situ* hybridization (WISH) was carried out using established protocols,[33] modified with a 5-min Proteinase K (Thermo Fisher) treatment to preserve neuromast integrity. The probes used were: *atoh1a*,[50] *notch3*,[48] *delta*,[50] *deltaD*,[50] *notch1a*, *kremen1*, *wnt2*, *ctnnb1*, *six1a*, *tnfsf10L3*, *sost*, *sfrp1a*, *lfng*, and *isl1a*. Antisense probes were generated using established protocols[33] or using a PCR-based protocol.[53]

HCR fluorescent RNA *in situ* hybridization

Hybridization chain reaction fluorescent *in situ* hybridization (FISH) was carried out following the manufacturer's protocol (Molecular Instruments). The probes used were *krm1*-B1(4 pmol) and *tnfsf10L3*-B2 (4 pmol), with the amplifiers B1-546 and B2-647 respectively (Molecular Instruments). Larvae were subsequently labeled with DAPI and mounted using Fluorescent Mounting Media (EMD Millipore) to prevent fading.

Immunohistochemistry and FM1-43FX labeling

Whole mount immunolabeling was performed using established protocols (Ungos et al., 2003).[54] The primary antibodies used were: anti-Oto-ferlin antibody (mouse monoclonal, 1:200, DSHB, University of Iowa), anti-Sox 2 antibody (rabbit polyclonal, 1:100, Invitrogen) and anti-BrdU antibody (mouse monoclonal, 1:100, BD Biosciences). Secondary antibodies used were: goat anti-rabbit Alexa 647 (1:1000, Invitrogen), goat anti-mouse Alexa 568 (1:1000, Invitrogen), and goat anti-mouse Alexa 647 (1:1000, Invitrogen). Mature hair cells were labeled by a 1-min incubation in 3μM FM1-43FX (Invitrogen).[55] Nuclei were labeled with 30μM DAPI (Thermo Fisher).

Neomycin exposure and regeneration

For hair cell ablation, 5 days post fertilization (dpf) larvae were incubated in 400 μM neomycin (*NEO*, Millipore-Sigma) for 0.5 h and then washed 3x in fresh embryo medium. In experiments analyzing complete regeneration, larvae were collected 3 days following *NEO* exposure. For RNA *in situ* hybridization, larvae were collected 4 h or 1 day post *NEO*. To assess multiples rounds of hair cell ablation and regeneration, larvae were exposed to *NEO* at 5dpf, 8dpf, 11dpf, and 14dpf; larvae were fixed 3 days after their final *NEO* exposure.

BrdU incorporation

Cellular proliferation during regeneration was analyzed using bromodeoxyuridine (BrdU; Millipore Sigma). BrdU incorporation was carried out using established protocols[56,57]; larvae were incubated in 10 mM BrdU for 24 h at set times following NEO-induced ablation: for 5–6 days BrdU, larvae were exposed to BrdU immediately after *NEO* for 24 and then transferred to fresh E3 for 2 days; for 6–7 days BrdU, larvae were kept in E3 for 1 day following *NEO*, then incubated in BrdU for 1 and transferred to E3 for 1 day; and for 7–8 days BrdU, larvae were kept in E3 for 2 days following *NEO* exposure, followed by 24 h BrdU incorporation. All larvae were collected for fixation at 8dpf.

Inhibitor treatment conditions

Wnt signaling was activated using the Gsk3β inhibitor 1-azakenpaullone (AZK; Millipore Sigma[38]) or was inhibited using the Tankyrase inhibitor IWR-1-endo (Millipore Sigma), both were dissolved in DMSO and diluted in E3 embryo medium to 9μM and 22μM respectively. Control larvae were incubated in less than 1% DMSO. Notch inhibition was done using the γ-secretase inhibitor LY411575 (Millipore Sigma) at 50μM with DMSO as a control. For regeneration experiments in the presence of inhibitors, 5 dpf larvae were treated with inhibitors or DMSO for 5 h prior to exposure to *NEO*. Following NEO-induced ablation, larvae were incubated in DMSO or inhibitors for 3 days of regeneration.

Photoconversion

For photoconversion experiments using *Tg(sost:nlsEos)^{w215}* or *Tg(sfrp1a:nlsEos)^{w217}* fish, 5 dpf larvae were placed in a shallow depression slide and exposed to 405 nm light for 20 s using a Zeiss Imager.D2 compound microscope and a 10× objective. For regeneration experiments, photoconversion was carried out prior to *NEO* exposure. For live imaging of *Tg(sost:nlsEos)^{w215}* fish, larvae were anesthetized using tricaine and embedded in 1.2% low melt agarose/E3 embryo medium.

Image collection

For imaging of RNA *in situ* hybridization and immunohistochemistry, processed larvae were placed in 50% glycerol/PBS and mounted on slides. For imaging of HCR *in situ* hybridization, larvae were mounted on slides in Fluorescent Mounting Media (Calbiochem) and imaged within 3 days of processing to prevent signal loss. Images were collected using a Zeiss 510 meta confocal microscope using Zen 2009 software.

Images were processed using Fiji software[49] and brightness and contrast were adjusted using Photoshop (Adobe). Neuromasts L1-L4 were analyzed for each fish and cells were manually counted under blinded conditions.

QUANTIFICATION AND STATISTICAL ANALYSIS

All statistical analysis was carried out using Graphpad Prism 10 (GraphPad Prism version 10.0.0 for Mac, GraphPad Software, San Diego, California USA, www.graphpad.com). A Mann-Whitney nonparametric test was used for pairwise comparisons and a Kruskal-Wallis test with Dunn's multiple comparison tests was used of all other data. Significance was set at $p < 0.05$. All data is presented as $\pm$ standard deviation (SD).